THE PHOTOCHEMICAL AND THERMAL OXIDATION OF HYDROGEN SULPHIDE

by

RONALD SIU-MAN TSE

B.A.Sc., University of Toronto, 1958

A THESIS SUBMITTED IN PARTIAL FULFILMENT OF THE REQUIREMENTS FOR THE DEGREE OF

MASTER OF SCIENCE
in the Department
of
CHEMISTRY

We accept this thesis as conforming to the required standard

THE UNIVERSITY OF BRITISH COLUMBIA

September, 1962

In presenting this thesis in partial fulfilment of the requirements for an advanced degree at the University of British Columbia, I agree that the Library shall make it freely available for reference and study. I further agree that permission for extensive copying of this thesis for scholarly purposes may be granted by the Head of my Department or by his representatives. It is understood that copying or publication of this thesis for financial gain shall not be allowed without my written permission.

Department of Chemistry

The University of British Columbia,
Vancouver 8, Canada.

Date Oct. 29, 62.

ABSTRACT

In order to elucidate the mechanism of hydrogen sulphide oxidation, the photo-oxidation and thermal oxidation of hydrogen sulphide were studied, using gas chromatography for the analysis of final products.

Photo-oxidation was studied at 130° and 150°C. Products found were sulphur dioxide, hydrogen, water and sulphur. Production of sulphur dioxide was found to be inhibited by an increase in surface area. Whether in photo- or thermal oxidation, the yield of sulphur dioxide increased drastically with slight increases in $(O_2)/(H_2S)$ ratio. This was also observed in the yield of hydrogen in photo-oxidation. Thermal oxidation was studied at 160°, 170°, 190°, 210°, 225°, 240°, and 260°C. Products were sulphur dioxide, water, and sulphur. No hydrogen was found. An expression for the production of sulphur dioxide was obtained:

$$\frac{\Delta(SO_2)}{\Delta t} = k(H_2S)^{-1 \rightarrow +1}(O_2)^3.$$

The overall activation energy was found to be 21.2±2k.cal./mole. Comparison with previously reported works was made and a mechanism proposed.

ACKNOWLEDGEMENT

I wish to express my sincere gratitude and thanks to Professor C.A. McDowell for his generous encouragement, supervision and enlightening discussions throughout the course of the work.

I am grateful to the University of British Columbia for Teaching Assistantships during the 1959-60, 1960-61, and 1961-62 sessions.

Finally, I wish to thank the glassblowing, electronic and mechanical workshop staff for their assistance in the construction of the apparatus.

CONTENTS

INTRODUCTION

There have been many investigations on the oxidation of hydrogen sulphide by oxygen. In each of these investigations, a certain special aspect of the reaction was studied, but no effort has been made to correlate these observations as a whole. Thompson and Kelland[28] studied the thermal oxidation at fairly high pressures and O_2:H_2S ratios. The activation energy was estimated to be in the range 18-20 k.cal./mole. The Russian group of Emanuel, Semenov et al[1-13] has made extensive studies on the thermal oxidation of hydrogen sulphide by oxygen. Their investigations were carried out at the temperature around 270° C but they did not analyse their products beyond taking the absorption spectrum of the intermediate (SO) and of the final product SO_2. They based most of their study on the measurement of pressure changes.

The results of Emanuel et al are nicely summarised in Semenov's paper[9]. At 270° C and an initial pressure of 100 mm. Hg maximum reaction rate was reached at 18-20% conversion. 50% conversion was reached after two minutes. The intermediate SO was identified by comparing the absorption spectrum of the intermediate with that of SO obtained by Schenk[14]. SO was found to dimerise when the temperature falls below 300° C.[9]. Some further study has been made by Emanuel et al on this dimerisation by measuring the pressure contraction on cooling[11]. They also

found[9] that at 270° C there was an induction period for the H_2S and O_2 reaction. During this induction period, which lasted about 20 seconds, only SO was formed. SO_2 was formed subsequently. After 40 seconds the conversion was found to be

$$80\%\ H_2S \longrightarrow SO$$

$$20\%\ H_2S \longrightarrow SO_2$$

Semenov[9] proposed the following mechanism, based on the results of Emanuel et al[1-13] : -

Primary	H_2S	+	O_2	→	H_2O	+	SO	
Chain Propagation	S	+	O_2	→	SO	+	O	- 0.8 k.cal.
	O	+	H_2S	→	H_2O	+	S	+ 45 k.cal.
Chain Branching	SO	+	O_2	→	SO_2	+	O	

Termination

S + wall

O + wall

Negative interaction step

$$SO + SO + O_2 \longrightarrow 2SO_2$$

The last step was used to explain the fact that maximum reaction rate occurred at 20% conversion.

Norrish and his collaborators studied the mechanism of hydrogen sulphide combustion with flash photolysis and kinetic spectroscopy[15,16]. An initial SH absorption spectrum was observed which gradually disappeared. The disappearance occurred much faster in the presence of O_2. In the presence of a large excess of inert gas, SO_2 was formed in a very small amount and S_2O_2 was the final pro-

duct which was stable even at high temperatures. When inert gas was not added, OH spectrum appeared on the disappearance of the SH spectrum. SO_2 was the final product and S_2O_2 was always absent. On flash irradiation both the spectra of S_2O_2 and of SO_2 disappeared temporarily. These authors proposed the following mechanism:

Initiation :

$$H_2S + h\nu \longrightarrow SH + H \qquad (1)$$

$$H + H_2S \longrightarrow SH + H_2 \qquad (2)$$

In the presence of a large excess of inert gas, chain termination :

$$SH + O_2 \longrightarrow SO + OH \qquad (3)$$

$$OH + SH \longrightarrow SO + H_2 \qquad (4)$$

$$SO + SO \longrightarrow S_2O_2 \qquad (5)$$

Flash irradiation of S_2O_2

$$S_2O_2 + h\nu \longrightarrow SO + SO \qquad (6)$$

$$SO + SO \longrightarrow S_2O_2 \qquad (5)$$

In the absence of inert gas

Chain propagation

$$SH + O_2 \longrightarrow SO_2 + O \qquad (3)$$

$$OH + H_2S \longrightarrow SH + H_2O \qquad (7)$$

Chain-branching

$$SO + O_2 \longrightarrow SO_2 + O \qquad (8)$$

$$O + H_2S \longrightarrow OH + SH \qquad (9)$$

Chain termination and light emission

$$SO + O \longrightarrow SO_2^{*} \longrightarrow SO_2 + h\nu \qquad (10)$$

Flash irradiation of SO_2

$$SO_2 + h\nu \longrightarrow SO_2^* \qquad (11)$$

$$SO_2 + SO_2 \longrightarrow SO + SO + O_2 \qquad (12)$$

$$SO + O_2 \longrightarrow SO_2 + O_2 \qquad (8)$$

$$O + SO \longrightarrow SO_2 \qquad (10)$$

The slow photo-decomposition of hydrogen sulphide and the slow photochemical reaction between hydrogen sulphide and oxygen have been studied by Darwent and Roberts[17] and by Darwent and Krasnansky[18], respectively. By gas burette methods, Darwent and Roberts[17] analysed only the H_2 produced. The quantum yield was shown to be close to unity and to be essentially independent of temperature, pressure, and light intensity. The thermal decomposition reaction was found to be heterogeneous at low temperatures and became homogeneous of the second order at 650° C. No decrease in rate was observed in the photolysis of H_2S in large excess of SF_6. The following mechanism was postulated by Darwent and Roberts[17] :

$$H_2S + h\nu \longrightarrow H + HS \qquad (1)$$

$$H + H_2S \longrightarrow H_2 + HS \qquad (2)$$

$$2HS \longrightarrow H_2S + S \qquad (3)$$

$$H + HS \xrightarrow{\text{fast}} H_2 + S \qquad (4)$$

$$2HS \longrightarrow H_2 + S_2 \qquad (5)$$

Reactions (1) and (2) are well established. Reaction (3) was found to be thermoneutral. Reactions (4) and (5) were used to explain the quantum yield being bigger than unity. Moreover, reaction (5) could explain the observation of S_2

bands in photochemically decomposing H_2S made by Porter[19] and by Ramsay[20]. The thermal reaction was considered by Darwent and Roberts as :

$$2H_2S \longrightarrow 2H_2 + S_2$$

In studying the photochemical reaction of hydrogen sulphide with oxygen, Darwent and Krasnansky[18] analysed only for H_2 and used gas burette methods. They correlated their results using the following postulated mechanism :-

$$H + HX \longrightarrow H_2 + X$$

$$H + O_2 \longrightarrow HO_2^*$$

$$HO_2^* \longrightarrow H + O_2$$

$$HO_2^* + M \longrightarrow HO_2 + M$$

$$HO_2^* + O_2 \longrightarrow H + 2O_2$$

The thermodynamically favourable reactions

$$HS + O_2 \longrightarrow H + SO_2$$

$$HS + HO_2 \longrightarrow H_2 + SO_2$$

$$H + HO_2 \longrightarrow 2OH$$

were found to disagree with experimental data.

It should be noted that Emanuel, Semenov et al[1-13] did not attempt to measure any possible production of hydrogen. The Zeelenberg proposal[16] included nearly all possible paths; but measurements were only made by kinetic spectroscopy. Darwent et al[17,18] practically ignored the SO_2 and H_2O produced.

Formation of sulphur has only been mentioned by Darwent and Krasnansky[18] and has not been taken into account

by other workers. Sulphur was observed by the aforementioned authors as a result of decomposition of H_2S or its oxidation. Moreover, it has long been known that when H_2S and SO_2 are brought together, sulphur is deposited.[21]

Another reaction which is of interest is the one between hydrogen and sulphur. This reaction has been shown to be mainly heterogeneous at low temperatures,[22] to have an activation energy of 26 k.cal. and thus thermodynamically favourable.

The present investigation was made in order to correlate all the previous data and to present a complete mechanism for the photochemical system of H_2S and O_2. An attempt was made to study the slow photochemical and thermal oxidation of hydrogen sulphide, analysing all the products by gas chromatography. It was hoped that the results would give a clarified picture of the mechanism of this complex reaction.

APPARATUS

The Vacuum System

The vacuum system (fig. 1) was of conventional design with modification in order to avoid mercury in the sample line. The traps between the diffusion pump and stopcock F were normally immersed in liquid nitrogen so that any mercury vapour from the diffusion pump, the McLeod Gauge and the Toepler pump could be collected between these cold traps. These traps were removable for cleaning. Whenever stopcock Y in the sample line was open, the cold trap preceeding stopcock A, in the sampling system was immersed in liquid nitrogen. One exception to this operation was when SO_2 was passed through Y into the gas burette. In such a case, Y would be open for only fractions of a second. Thus virtually no mercury vapour could enter the sample line.

The vacuum system was constructed with pyrex glass with the exception of the reaction cell, which was made of fused quartz with optically plane end windows. The mechanical pump was a Welch No. 1400, "Duo Seal" two-stage oil pump. The diffusion pump was homemade but of usual design. The trap between the diffusion and mechanical pumps was used to collect and drain bounced off mercury drops. The main vacuum line was 22 millimetres in diameter and the sample line 12 millimetres. The lead to the spiral gauge was of 2 millimetres capillary and those from the cell to the gas chromotograph system were also capillary tubing.

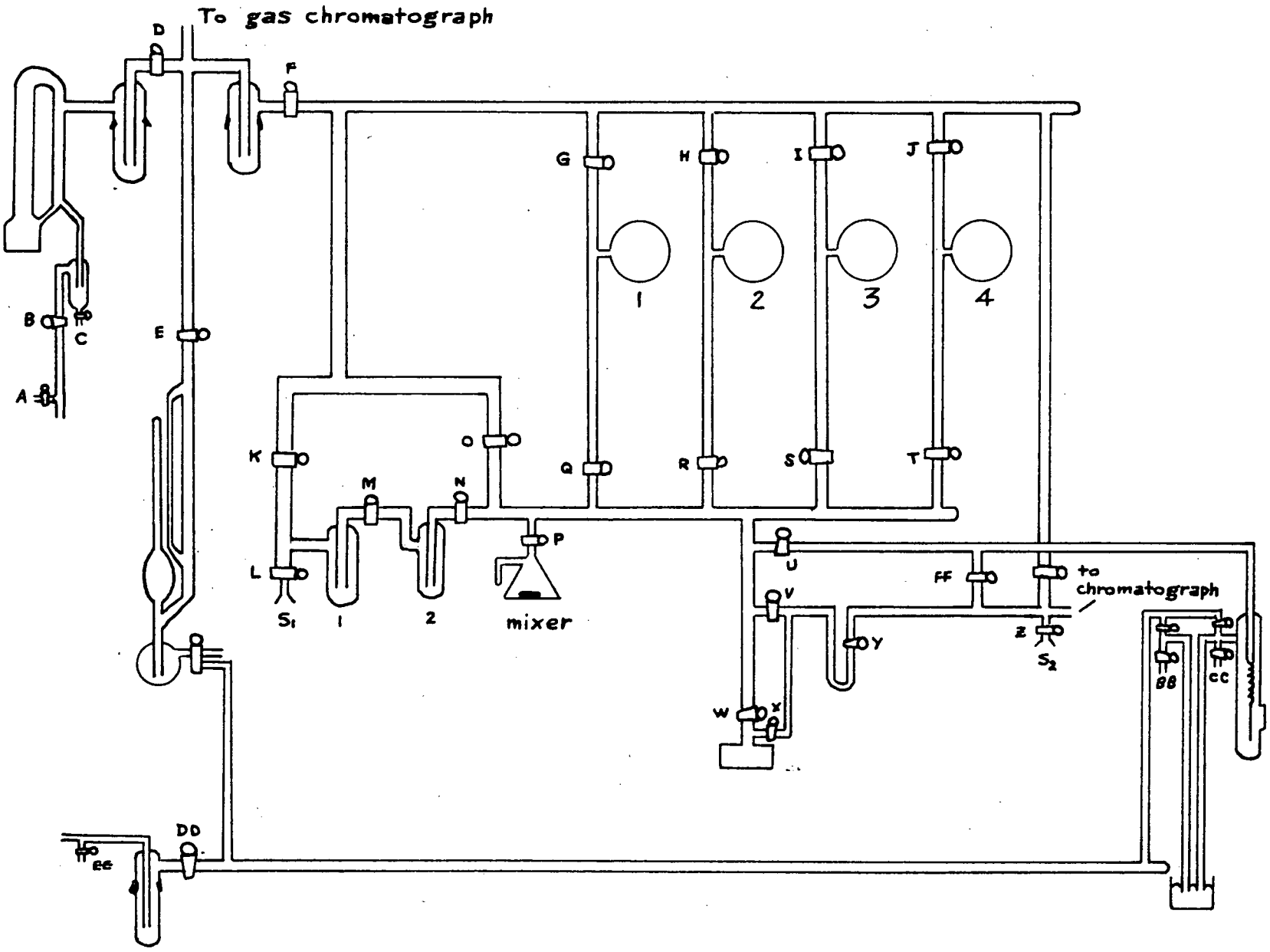

fig. 1. Main Vacuum System

Stopcocks were generally lubricated with Apiezon L grease. Those close to the furnace were lubricated with Apiezon N grease. It was found unnecessary to use high temperature grease. In this system a vacuum of 10^{-5} millimetre Hg at the McLeod gauge could readily be obtained. Dark discharge of the Tesler coil was easily reached elsewhere except in the spiral gauge leads.

The mixing vessel was made out from a 125 millilitre Erlenmeyer flask. The total volume was 148 c.c. A magnet enclosed in pyrex was placed inside while a Precision Scientific Co. "Mag-mix" was placed under the flask. The speed of stirring could be controlled on the "Mag-mix".

The spiral gauge had a sensitivity of 0.840 millimetres on the scale /1 millimetre Hg and could withstand 1 atmosphere on both sides. The calibration curve for the spiral gauge is shown on fig. 2. More sensitive spirals with a smaller range had been tried but found to be too fragile. It was possible to read 0.5 millimetre on the spiral gauge scale.

Optically plane windows were fused to the ends of the unpacked quartz cell. The internal measurements were 100 millimetres in length and 37 millimetres in diameter. The volume was 107.5 c.c. and the dead volume in the lead to the cell was 8.5 c.c.

The internal dimensions of the packed cell was 100 millimetres in length and 28 millimetres in diameter. It was packed with 100 quartz rods of 83 millimetres long and

fig 2 CALIBRATION of SPIRAL GAUGE

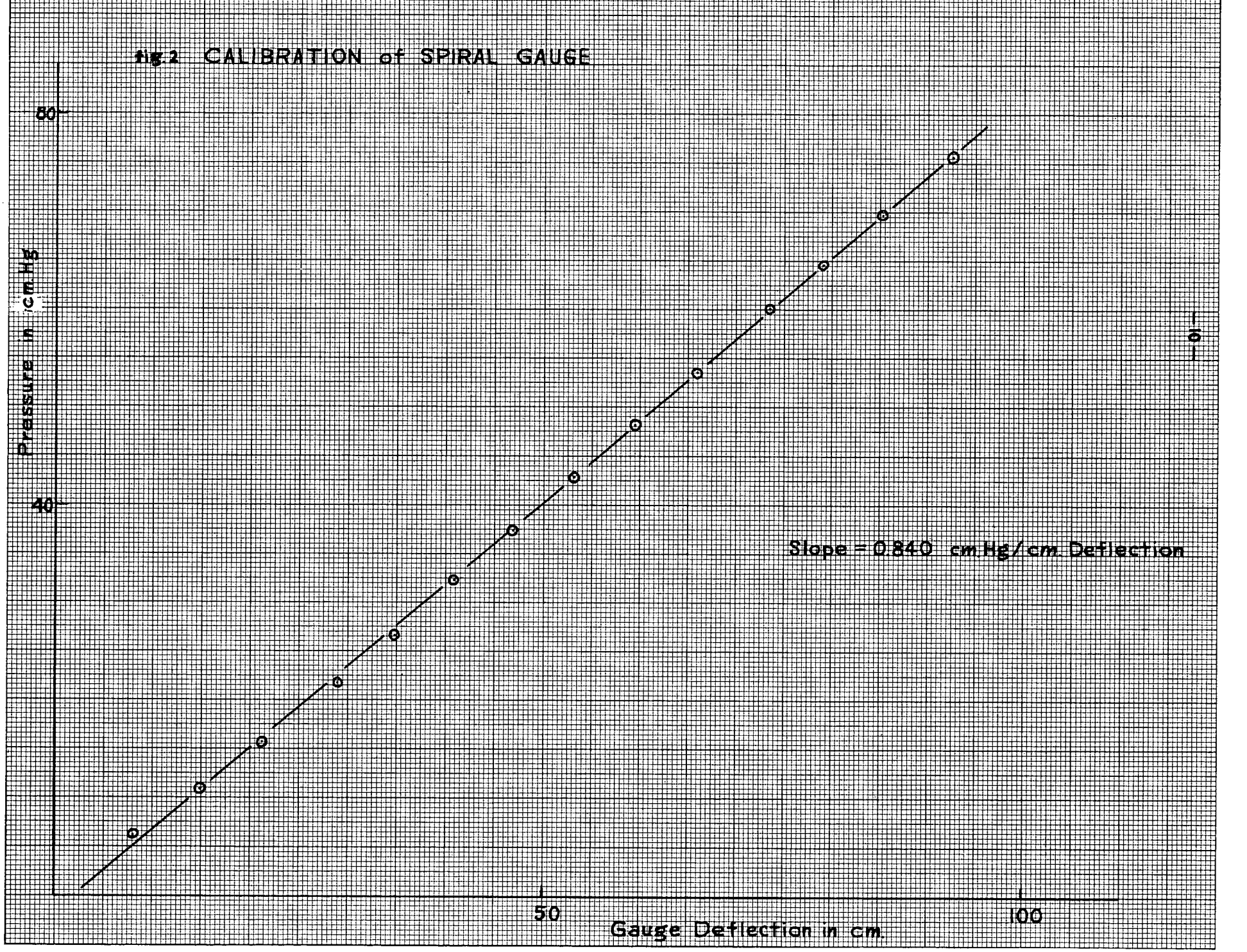

2 millimetres in diameter. The free volume was 35.4 ccc. The dead volume in the lead was 3.6 ccc. The surface to volume ratio was 4.3 excluding dead space and 4.5 including the dead volume.

Referring to the admission system of the gas chromatograph (fig.3) the volume of the gas burette was 28.7ccc. It was found that after 3 operations of the Toepler pump, 94% of the material in the reaction cell could be transferred to the gas burette. It was also found that the volume of the sample line, defined by stopcocks N,O,P,Q, R,S,T,U,V,W, was 109.5 ccc.; the volume defined by V,X,Y was 5.6 ccc.; that defined by Y,Z,AA,A' was 20.4 ccc.; the volume defined by C',D',E',F' was 4.3 ccc.

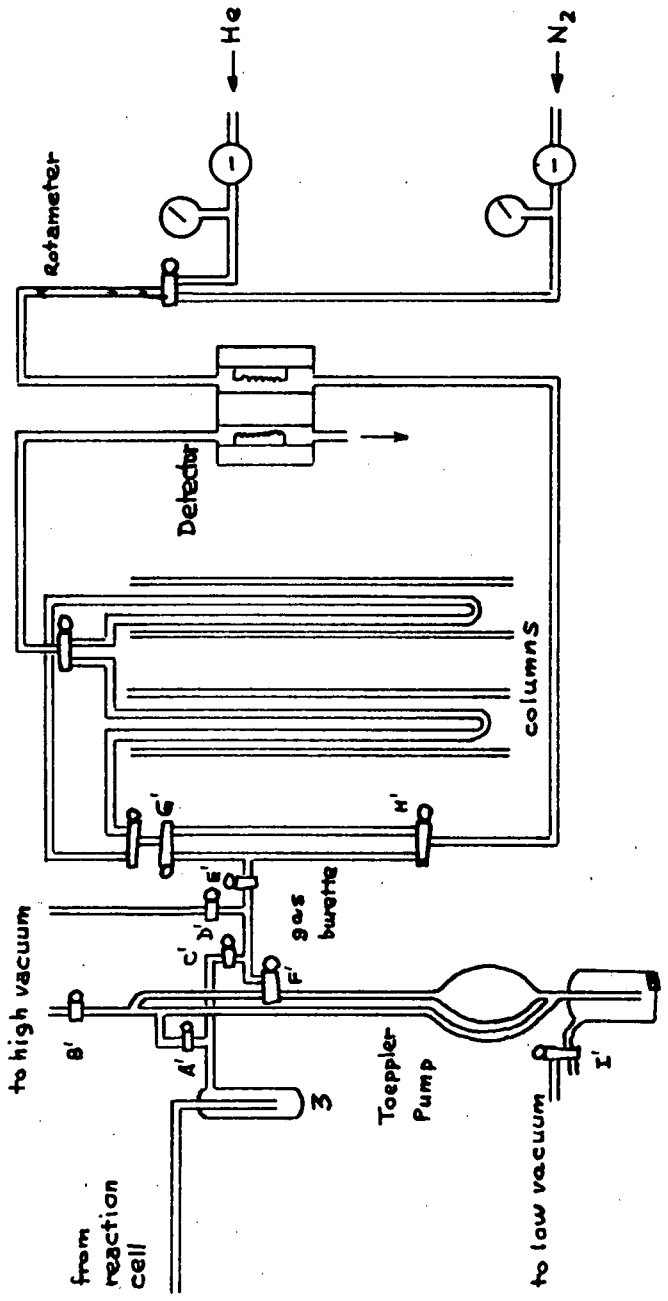

fig. 3. Gas Chromatographic System

The Gas Chromatographic system

The gas chromatographic system is represented in fig. 3. From the rotameter onwards, it was constructed with pyrex. Carrier gas from commercial cylinders was first reduced to 20 p.s.i.g. before entering a Matheson pancake type low pressure regulator in which the pressure was furthur reduced to 5 p.s.i.g. for helium and 9 p.s.i.g. for nitrogen. Trap 3 was usually immersed in dry ice to collect any water from the cylinders. A rotometer (No. G 9142 B manufactured by the Monostat Corp., New York) placed between the low pressure regulator and the thermal conductivity cell, was used to indicate the flow.

The thermal conductivity cell was identical with the one designed by Ryce, Kebarle and Bryce[23]. The only difference was that the filaments were a pair of matched tungsten coils of 20Ω each made by Gow-mac Instrument Co., Madison, N.J. It was found that the tungsten filaments were even more stable and more sensitive than platinum filaments. The cell block was wrapped with heating tape and placed in an insulated can. Temperature was kept at about 40°C. The cell block itself was grounded.

The gas burette was made of 15 millimetres tubing to ensure quick mixing. The leads were usually 8 millimetres in diameter. The lead from the columns to the thermal conductivity cell were wrapped with heating tape. The chromatographic columns were made of 6 millimeters tubing and 8½ feet long. These were connected to the system through No. 12 ball joints, lubricated with Apiezon L grease or silicone grease according to temperature. Temperature of the chromatographic columns was controlled by heating coils placed inside a large glass tube. An even larger glass tube fitted over the first one providing adequate insulation. Ends of this double-layer tube were plugged with glass wool to prevent convection.

A few chromatographic packing materials had been tried, namely, silica Gel, Perkin-Elmer Column W material, T.C.P. on Celite 545, activated charcoal, and P-0190 on acid washed chromosorb manufactured by F & M Scientific Corporation, Wilmington, Delaware. At room temperature, silica gel separated very well H_2S from O_2 but poorly H_2S from SO_2. It also irreversibly absorbed H_2O. The Perkin-Elmer material was supposed to give symmetric peaks for polar materials such as H_2O but its sensitivity was lower than that of the F. & M. material. T.C.P. on Celite 545 would be good in separating organo-sulphur compounds[24] but did not give a good H_2O peak. In this in-

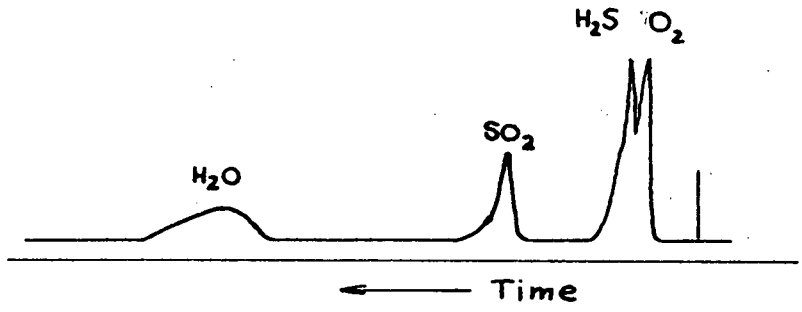

Column : F & M P-0190.

Temperature : 90°C.

Carrier gas : He

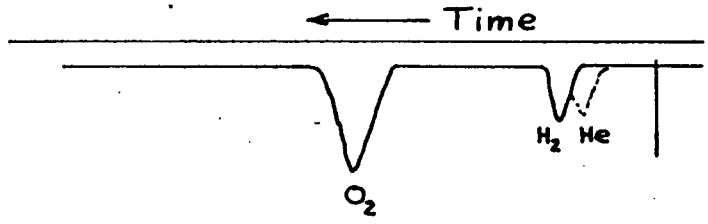

Column : B.D.H. activated charcoal, 50-200 mesh.

Temperature : Room.

Carrier gas : N_2

fig. 4

vestigation the useful property of the T.C.P. material was not needed.

After a few trials, the F. &. M Corp. P-0190 material with helium carrier gas was used to analyse SO_2 and H_2O. Operating temperature was set at about 90^oC, flow rate at 5.05 centimetres of the rotameter equivalent to 32.0 ml./minutes, and pressure at 5 p.s.i.g. Under these conditions hydrogen could be separated from oxygen and the oxygen peak usually overlapped the H_2S peak. The SO_2 and H_2O peaks were far separated from the H_2S and O_2 peaks. (fig. 4). With a chart speed of 30 inches per hour, O_2 appeared at 18 millimetres, H_2S at 25 millimetres, SO_2 at 56 millimetres, and H_2O at 23 centimetres. The tail for the H_2O peak was considerable. The sensitivity of analysis was 1.095×10^{-5} gm. mole of SO_2 in the unpacked cell per square inch on the recorder chart. It was possible to measure to 0.01 $inches^2$. Due to the tendency of H_2O adhering to the walls of tubings, the calibration for H_2O in this column was not consistent. But the value was about 3.28×10^{-5} gm. mole in the unpacked cell per square inch on the recorder chart.

The activated charcoal used to analyse hydrogen with nitrogen as carrier gas was B.D.H. AR grade charcoal of 50-200 mesh. The optimum operating conditions were found to be the following : pressure= 9 p.s.i.g.; temperature= room temperature, but column in insulating enclosure as the F. & M. P-0190 column; flow rate= 4.0 centimetres on

the rotameter, equivalent to 9.8 millilitres per minute. Higher temperature would speed up the separation but sensitivity would drop considerably. The relatively high pressure was needed due to the fine particle size of charcoal. Two columns were found suitable, one 8½ feet long and the other 5 feet long. The long column gave a sensitivity of 4.88×10^{-6} gm. mole/inches^2 for hydrogen and1.725×10^{-4} gm. mole/inches^2 for oxygen. The short one had 6.99×10^{-6} gm. mole/inches^2 for hydrogen and 2.87×10^{-4} gm. mole/inches^2 for oxygen. For better sensitivity, the long column was usually used. With the same recorder chart speed of 30 inches per hour, hydrogen appeared at 37 millimetres, Helium at 34 millimetres and oxygen at 91 millimetres. Hydrogen and helium peaks overlapped each other, but in any run, the helium from a previous analysis was completely driven out by the nitrogen carrier gas before any hydrogen was admitted to the system.

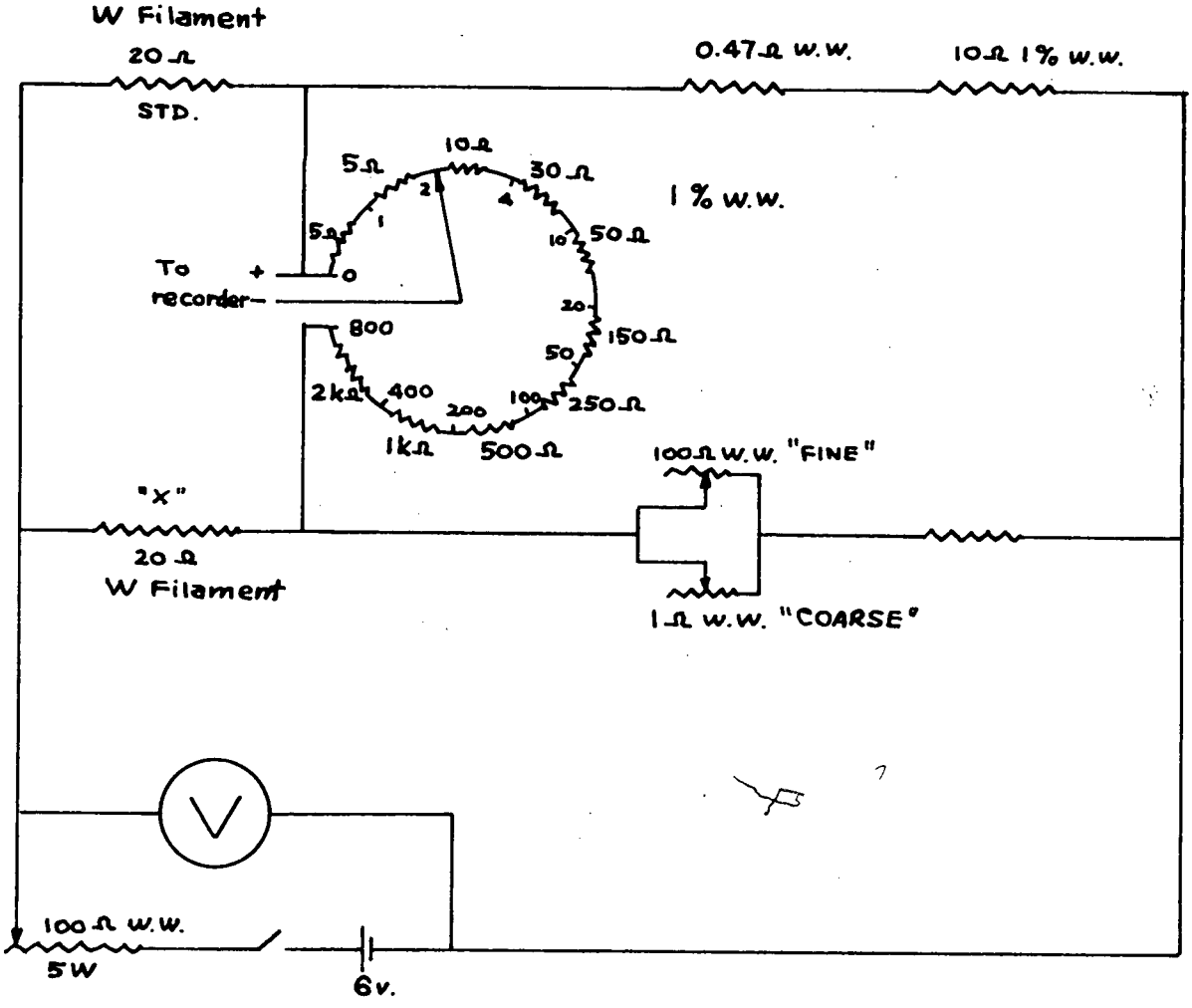

fig. 5 Circuit Diagram for

Thermal Conductivity Cell

Thermal Conductivity Cell Detector System : -

Fig. 5 is a schematic diagram of the electrical circuit for the thermal conductivity detector of the gas chromatographic system. The matched 20Ω tungsten filaments formed half of a conventional Wheatstone bridge. The other half was composed of a pair of precision, temperature constant 10Ω wire-wound resistors and other resistors for control purposes. 6 volts D.C. from an accumulator was usually applied across the bridge. The 0.47Ω W.W. resistor was used to unbalance the circuit so that a wide enough range of inequilibrium could be controlled.The controls were made up of a 100Ω and a 1Ω variable resistor in parallel, the 100Ω being the "FINE" control and the 1Ω the "COARSE" control. These controls were used to place the base line of the recorder at a desirable position on the chart.

In place of the galvanometer, a number of 1% precision and temperature constant wire wound resistors were mounted on a multiple switch plate. Various potentials could be taken to the recorder. This multiple switch provided steps of sensitivity 0,1,2,4,10,20,50,100,200,400 and 800, the last one being the most sensitive. The recorder used was a Leeds & Northrop Series 60000 type with a range of 0-10 m.v. Chart speed was set at 30 inches/hour.

The Mercury Arc

The lamp (fig. 6) used for photolyses was a U-shaped Hanovia D-88A-45 low pressure mercury arc. Approximately 94% of the intensity was the unreversed 2537A°. No filter was necessary.

The arc was put inside a tubular housing. A hole of about 1 centimetre in diameter allowed the light to pass into the optical system. The size of this hole could be varied by rotating a disc in which there were a set of holes of various size and which covered the hole on the lamp housing. The lamp was so aligned that this hole and the two limbs of the U-shaped arc were linear to allow maximum emitted intensity in this direction.

In order to keep the lamp temperature low for maximum 2537A° radiation, the lamp housing was wrapped with copper tubing in which cold water was passed. Cold air was blown from the bottom of the lamp housing and was allowed to escape mainly from the top. In such an arrangement, there was a danger of mercury condensing around the area opposite the opening to the optical system. To prevent this, a small amount of hot air was blown through a jet directly at this area. Flow rate of cold water was regulated by letting free flow from a can placed at a constant height.

Power supply to the lamp terminals was through a Sorensen voltage regulator. With the above mentioned arrangement, approximately 0.5 % stability over a few hours

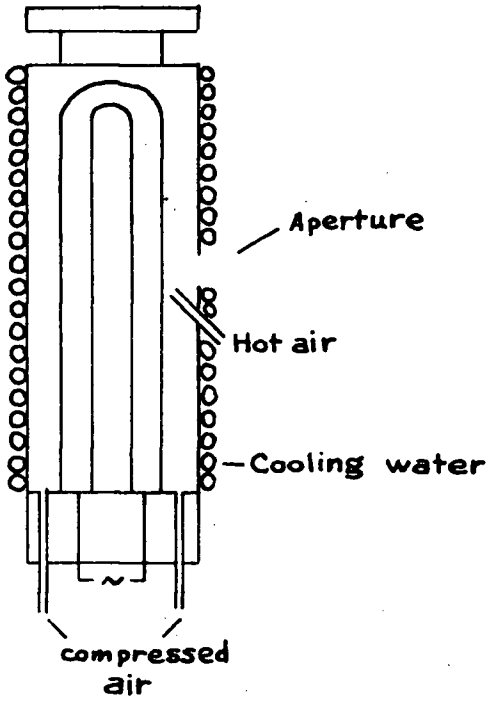

fig. 6

Low Pressure Hg Arc

Hanovia D-88A-45

with Housing

Medium Pressure Hg Arc

Hanovia SH-100

with Housing

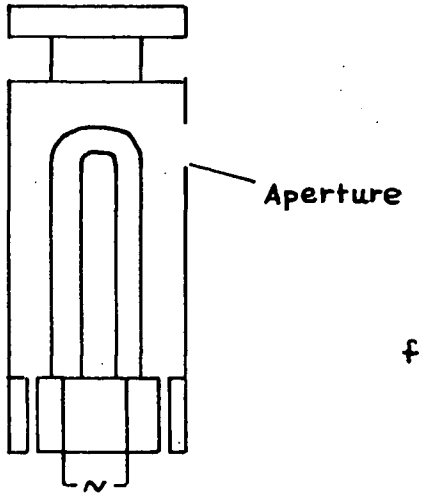

fig. 7

was always obtained. It was found that intensity greatly depended on the temperature of the mercury arc.

In the preliminary experiments, radiation of 3130 A^{o} was tried. For this wave length, a Hanovia SH 100 U-shaped high pressure mercury arc was used. The housing for this lamp is shown in fig. 7. Cold air was blown from the bottom of the housing to keep the lamp and environment from excess heat. A filter combination for 3130 A^{o} described by Kasha[25a] and by Hunt & Davis[25b] was used in conjunction with this lamp.

The Optical Bench

Fig. 8 shows schematically the arrangement of the optical bench. Radiation from the mercury lamp was colimated by two plano-convex lenses. The first one, with a focal length of 7.5 centimetres was placed 11.0 centimetres from the opening in the lamp housing. The second one, mounted on the furnace, was 23.55 centimetres from the first one. The focal length of this second lens was 10.0 centimetres. The light beam was thus made approximately parallel.. Another plano-convex lens of 7.5 centimetres focal length was placed at the other end of the furnace and focussed the beam to a photocell. When filters were used, they were placed on a stand immediately behind the first lens. A shutter, made of aluminum sheet and operated by manually lifting it, was mounted on this stand. The

The whole optical system was enclosed in thin aluminum sheets and was almost light tight.

The Photometer

The circuit diagram of the photometer is shown in **fig. 9.**

fig. 9 a) Photocell. The photocell used was a British Cintel QVA 39 with a quartz envelope designed for the U.V. range. It was claimed to give an output proportional to the intensity of light shone on it. A curve representing relative sensitivity vs. wavelength of incident radiation is shown on fig. 10. and on fig. 11 the linearity of response with a fixed wavelength light is shown. No. 935 photocell could also be used with this photometer circuit, but the sensitivity of this photocell at 2537 A^{o} was very poor.

b) Operation. The photocell current passed through the resistor chain R 1-4 and the required voltage was tapped off with the selector switch S_1. An opposing voltage was then applied by the potentiometer circuit consisting of the battery B_1 and the series of dual decades R 5-12. B_1 was normally 2V and the voltage tapped from the potentiometer was adjustable to any value between 0 and 2V with an accuracy of 1×10^{-4} volts.

The difference between the voltage tapped from the resistor chain R 1-4 and the opposing voltage from the potentiometer was applied to the double triode amplifier valve V. The second triode unit compensated for supply voltage variation. The output of the amplifier was then

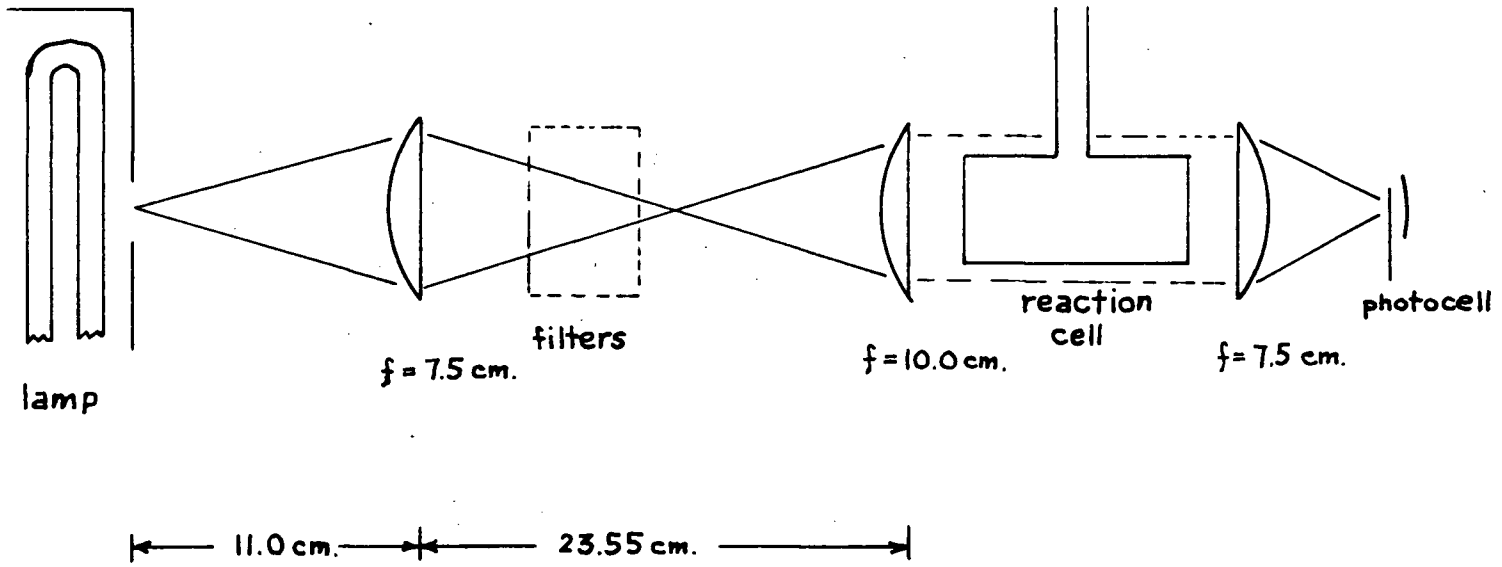

fig. 8 The Optical Bench

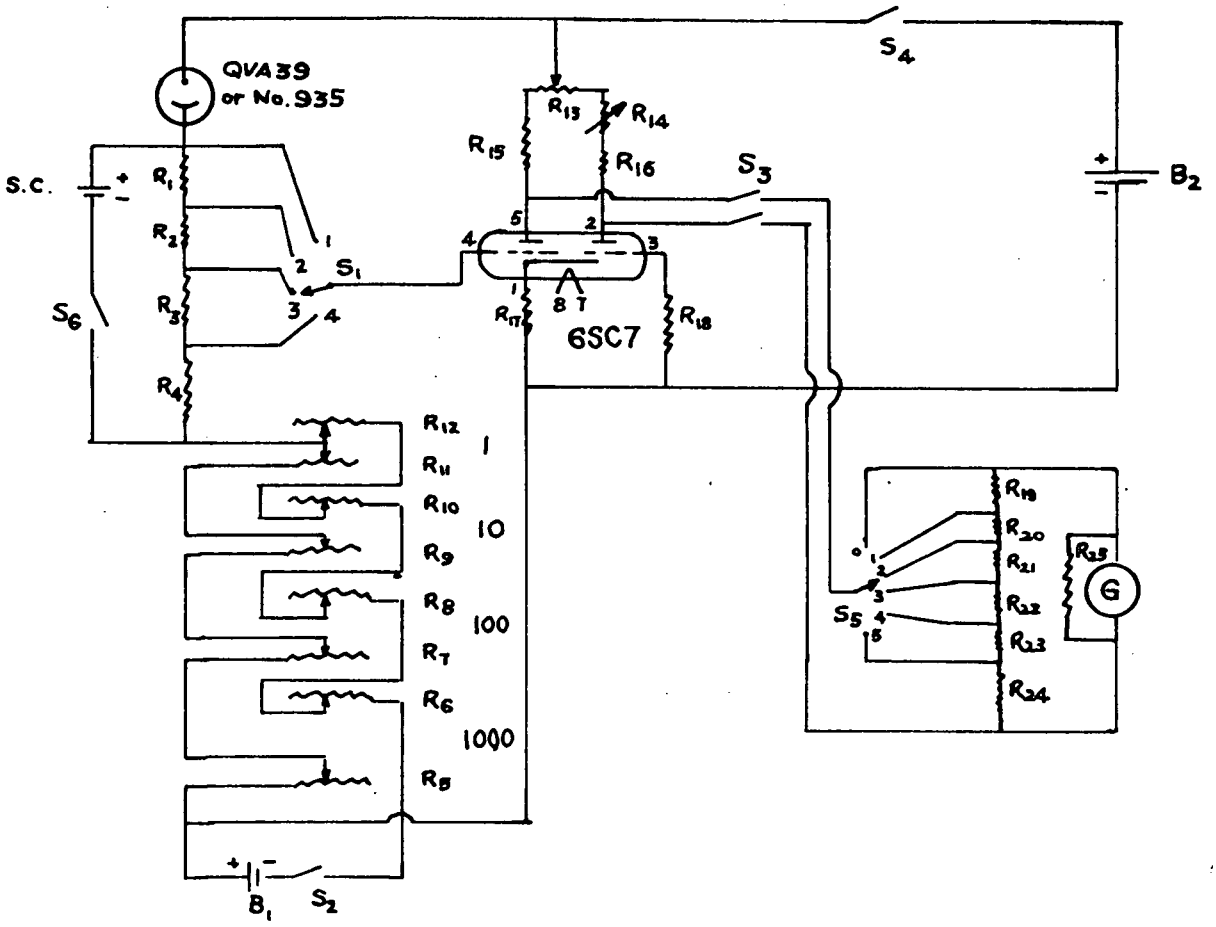

B_1	2v Accumulator	R_{13}	25k w.w. pot.
B_2	120v. h.t. battery	R_{14}	2k w.w. pot.
G	Galvanometer	R_{15}	50K w.w. lw.
S.C.	Standard Cell	R_{16}	50k w.w. lw.
R_1	5M h.s.c. lw.	R_{17}	2.2k w.w. lw.
R_2	1.5M h.s.c. lw.	R_{18}	1M ½w.
R_3	500k h.s.c. lw.	R_{19}	100k. w.w. lw.
R_4	150k h.s.c. lw.	R_{20}	33k w.w. lw.
$R_{5,6}$	10k dual decade	R_{21}	10k. w.w. lw.
$R_{7,8}$	1k dual decade	R_{22}	3.3k w.w. lw.
$R_{9,10}$	100 dual decade	R_{23}	1k w.w. lw.
$R_{11,12}$	10 dual decade	R_{24}	330 w.w. lw.
		R_{25}	10k w.w. lw.

fig. 9. PHOTOMETER CIRCUIT

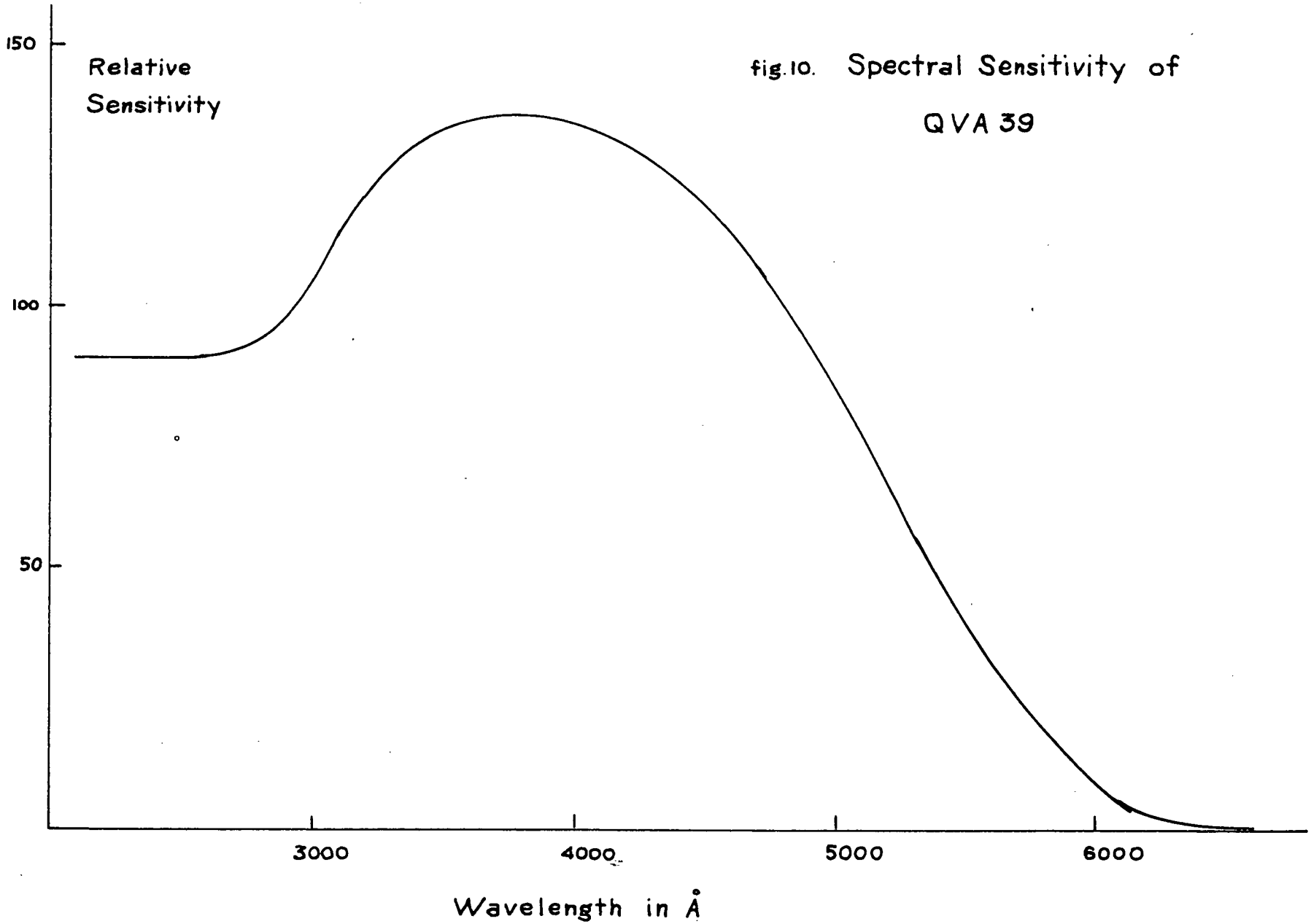

fig.10. Spectral Sensitivity of QVA 39

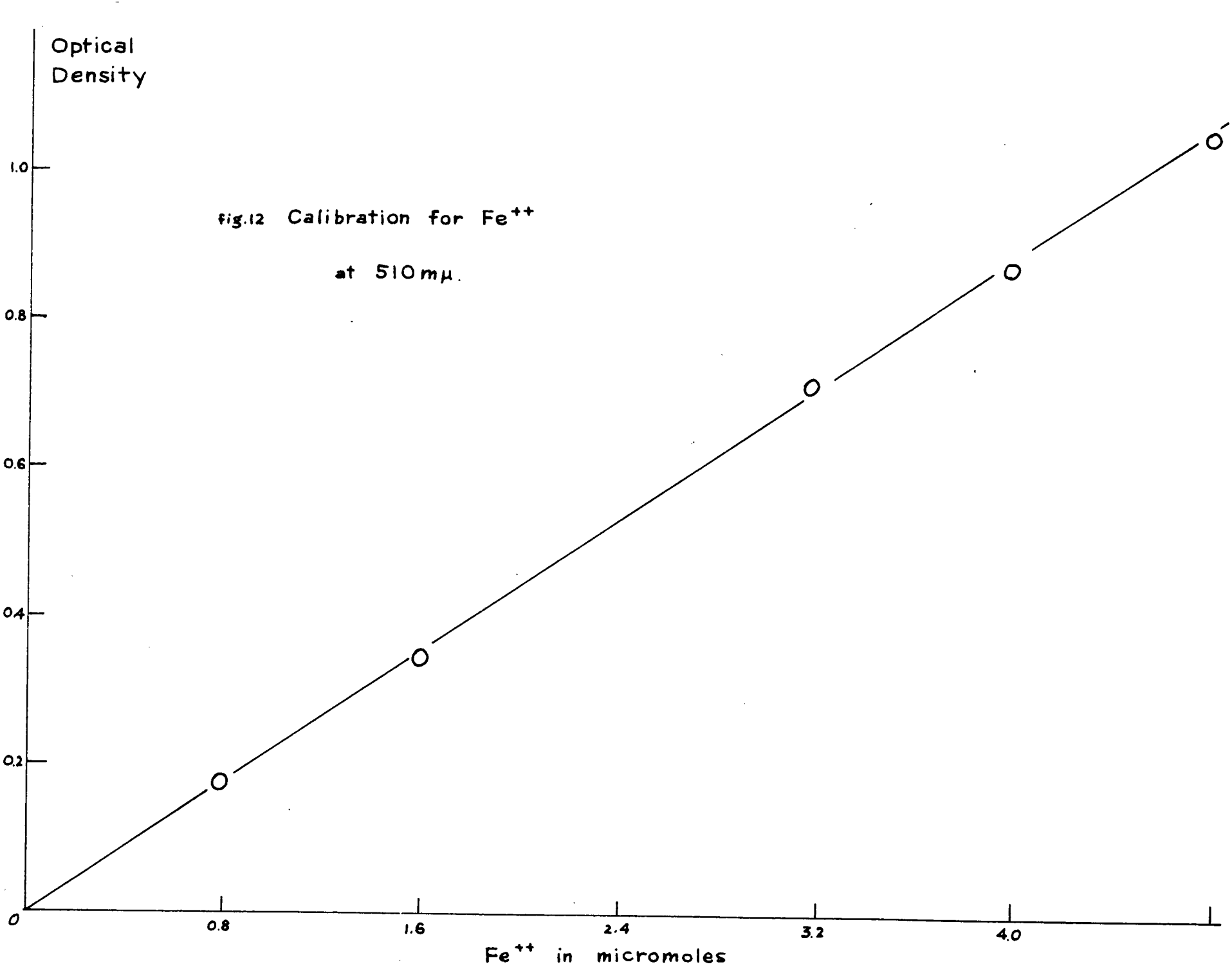

fig.12 Calibration for Fe^{++} at 510 mμ.

fed into the galvanometer G via the altenuator R_{19-24}. The galvanometer used was a Rubicon Catalogue No. 3402 and had a sensitivity of 0.046mA./mm. delfection. The high tension of the unit was derived from a 120 V. battery. Filament current of the valve 6SC7 was supplied by a 6v accumulator for maximum stability.

c)Photometric measurements.

In the actual apparatus, switches S_2, S_3 and S_4 and the switch for the filament current were mounted on a single 4-decked switch. S_1 was set at the 4 position. S_5 was usually set at position 3.

In order to operate the photometer, the instrument was turned on by closing the main switch and was allowed to warm up for about 15 minutes.

With no light falling on the photocell and the dual-decade potentiometer reading zero, the dark current from the photocell was balanced by adjusting R_{13} and R_{14} for zero galvanometer current. The circuit must be rebalanced for each position of the selector switch S_1.

S_6 was then closed, thus applying a standard voltage across the resistor chain R_{1-4}. The potentiometer voltage was then increased until the galvanometer showed zero deflection and the potentiometer reading taken. This operation was carried out to ensure that B_1 gave a constant voltage. The standard cell used was a SRIC miniature Eppley standard cell manufactured by the Sensitive Research Instrument Corporation, New Rochelle, N.Y. The e.m.f. of this standard cell was 1.0192 volts at 25°C.

S_6 was then opened and light was allowed to fall on the photocell. The potentiometer was adjusted so that the galvanometer showed zero deflection and the potentiometer reading taken. Assuming that the photocell characteristic was linear, this potentiometer readingwas proportional to the light intensity.

This unit was used to monitor the amount of light passing the reaction cell, both when empty and when filled.

d) Actinometry

A potassium ferioxalate actinometer was used according to Hatchard and Parker[29].

(1) Calibration for Ferrous Ion.

Four ml of the standardized 0.1M Ferrous sulphate solution was diluted to 500 ml with 0.1N sulphuric acid. The resulting solution contained 0.8×10^{-6} moles Fe per c.c. Next, 0,1,2,4, and 6 ml aliquots of this solution were added to individual 50 ml volumetric flasks. A sufficient volume of 0.1N sulphuric acid was then added to each flask to make the total volume of acid equal to 25 ml. Five ml of the 0.1% 1:10 phenanthroline solution and 12.5 ml of the buffer solution(600 ml of 1N sodium acetate and 360 ml 1N sulphuric acid diluted to 1 litre.) were then added to each flask. The flasks were diluted to volume with distilled water and allowed to stand for $\frac{1}{2}$ hour. At the end of this time, the optical densities of the developed solutions were measured at 510 m on a Unicam Sp. 600 spectrophotometer. A plot of the resulting optical densities against the ferrous ion concentration is shown in fig. 12.

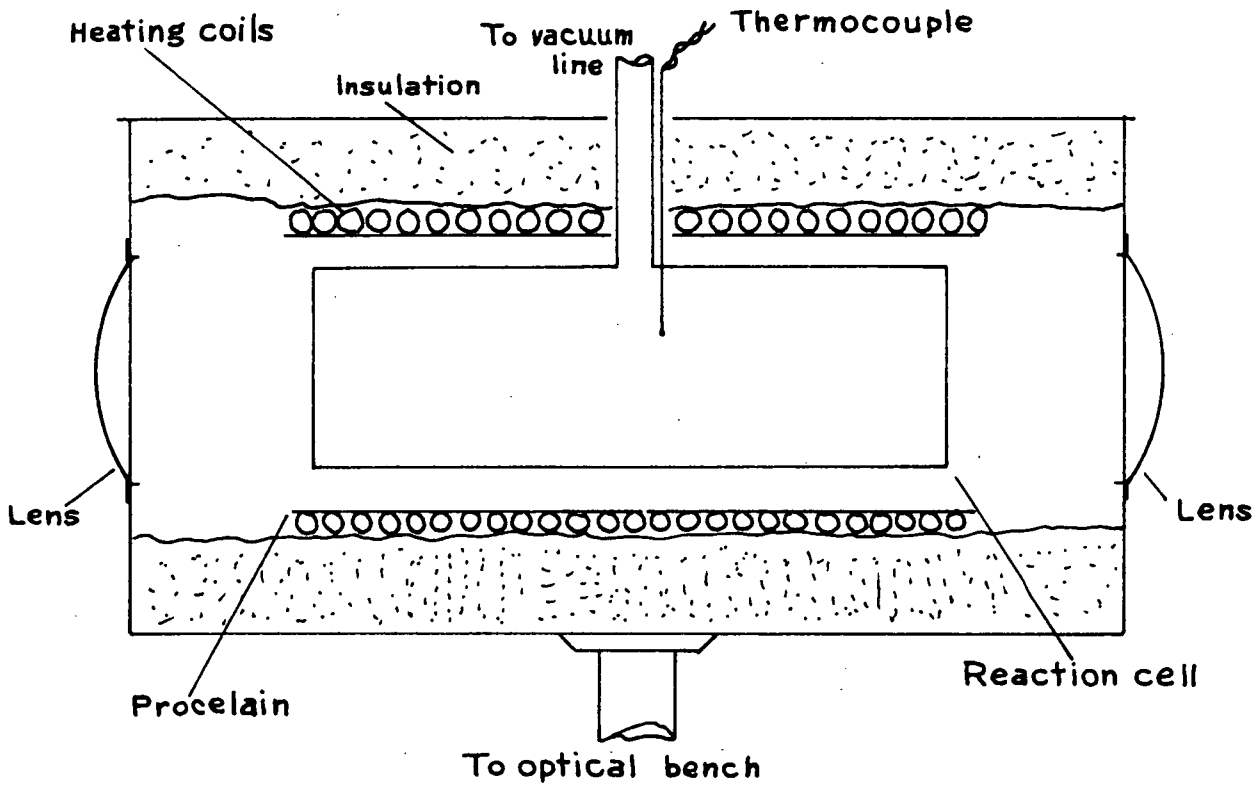

fig. 13 Furnace

(2) Calibration of Photometer

Both the lamp and photometer were warmed up. An intensity reading was made by the photometer. The photocell was then replaced by a 1 cm. thick quartz cell of about 10 ml capacity containing standard potassium ferrioxalate solution. This cell was covered with black tape except the windown facing the origin of light. This solution was irradiated for about six hours. At this time the photocell was replaced and another reading of light intensity taken. From the initial and final readings, an average value was obtained.

After irradiation, the actinometer solution was transferred to a 50 ml red coloured flask and 5 ml of the phenanthroline solution and 5 ml of the buffer solution were added. The volume was then made up to 50 ml with distilled water and the flask was allowed to stand for $\frac{1}{2}$ hour. This optical density of the resulting solution was then measured on the Unical at a wavelength of 510 mμ . The resulting optical density was then converted to micro moles of ferrous ion produced. The above procedure was carried out in duplicate and blanks were run along with each determination.

This calibration produced a value of 6.13×10^{10} quanta per ohm-second or 6.11×10^{-12} einsteins per Ohm-minute for the No. 935 phototube and 2.42×10^{-12} einsteins per Ohm-minute for the QVA 39 phototube.

The Furnace

Fig. 13 shows schematic diagram of the furnace arrangement. The furnace block itself was a hollow porcelain cylinder of 5.5 cm internal diameter. On the outside of this cylinder were grooves over which coiled heating elements were around. The block was split traversely in its centre to facilitate easy removal of the reaction cell. The heating coils were made of nichrome wires. The room temperature resistance of each half was about 28Ω . This furnace block rested on asbestos and Vermiculite insulation material which in turn was put inside a rectangular metal box with circular openings on each end over which plano-convex lenses were mounted. Glass wool was used as insulation over the furnace block. An aluminum sheet formed the cover of the external metal box. It was found easy to maintain $\pm$ 0.5^{o}C at 150^{o}C over a period of a few hours with a variac setting of about 30V applied to each half of the furnace heating coils. The thermocouple tip was glued to the reaction vessel with G. E. Glyptal cement. The whole furnace block was mounted on standard optical bench equipment and placed in the optical path as previously described in the section on the Optical system.

Thermocouple Circuit

Temperature measurements were made with copper-constantan thermocouples. A common cold junction was placed in a slush of ice and water in a Dewar flask.

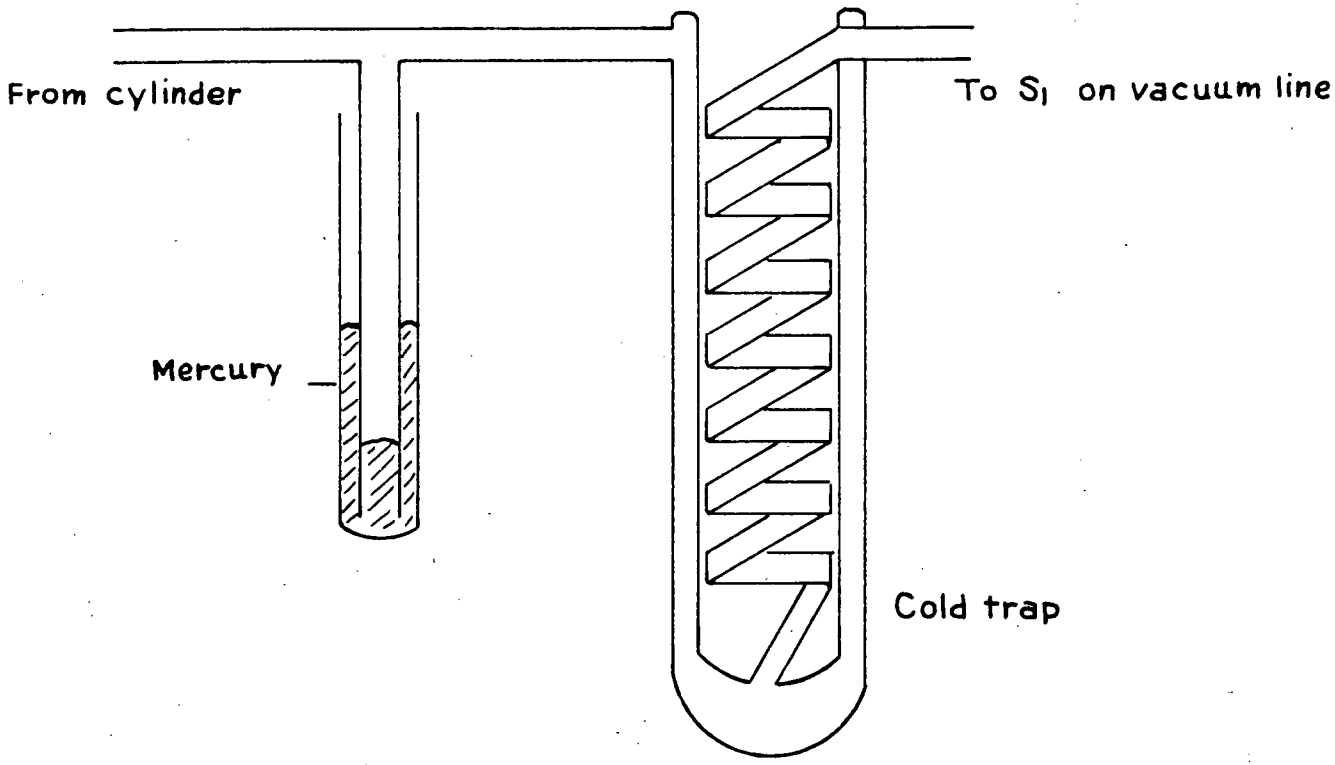

fig. 14 Gas admission system for oxygen

E.M.F. measurements were made with a Rubicon Type S potentiometer with a homemade chassis of controls as shown in fig. 15. In this potentiometer, two ranges were provided namely, 0-1.6 volts and 0-16 millivolts. Each range was coveredby two measuring dials, the first of which was composed of a 16 position switch controlling 15 fixed 10-Ω standard resistors, and the second of which was comprised of a 14-inch slide wire with 200 divisions. On the upper range, 15 increments of 0.1 volt each were developed across the first dial resistors, the slide wire affording continuous variation throughout at 0.1 volt intervals with 0.0005 volt each. On the lower range, the corresponding values were 1/100 of the foregoing. Thus it was possible to measure down to 0.001 of a millivolt.

Calibration of the potentiometer was made by setting switch S_2 to the standard cell position and closing S_1. Range connection was made to 1.6 volt and dials A and B were set to the standard cell value. Key k_1 was tapped and the "COARSE" and "FINE" resistors were adjusted to give a zero galvanometer reading, K_2 was then tapped for a finer calibration. To make thermocouple e.m.f. measurement, the switch S_2 was set to the E.M.F. position and the range connection was made to the 0.016 v. terminal. Having previously connected all the cold sides of the thermocouples to the terminal marked " - ", the selector switch was then set to the + terminal of the thermocouples in question. K_1 was tapped and dials A and B on the potentiometer ad-

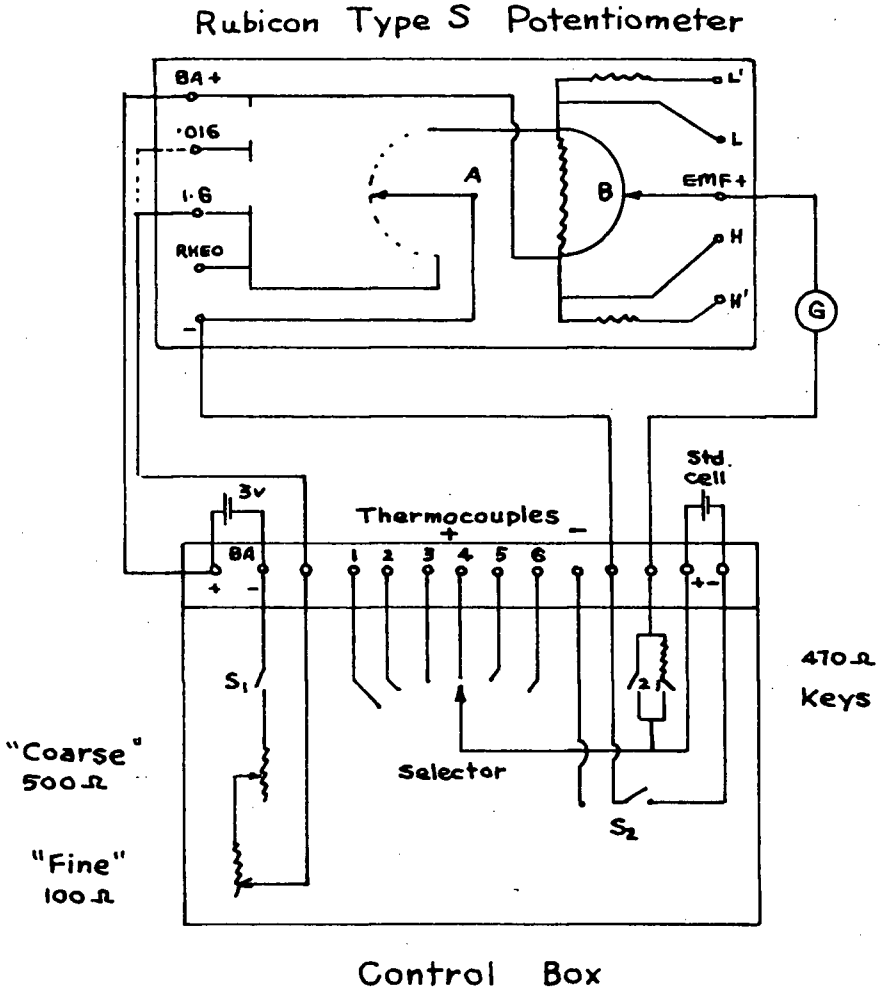

fig. 15 Thermocouple Potentiomter Circuit

justed to give a zero galvanometer reading. Then K_2 was tapped to give a more accurate reading.

Values of e.m.f. vs. temperature was taken from the Handbook of Physics and Chemistry, the 41st edition[26]. No actual calibration was done since temperature measurements were made to $\pm$ 0.5°C.

MATERIAL

Hydrogen Sulphide

Hydrogen Sulphide was obtained from commercial cylinders by Matheson Co. Only CP grade was available. The gas was subjected to purification as follows:
A needle valve was fitted to the cylinder and a tygon tubing with a B10 cone was joined to socket S_2 in the vacuum system. The tygon tubing was filled with H_2S by gently releasing the needle valve on the cylinder, and then the gas was pumped away by opening stopcock L. This was repeated twice to drive away any undesired gas in the tygon tubing. Having the system evacuated and all stopcocks along the sample line closed except M,N,S, & U, trap 1 was cooled in a slush of dry ice and acetone. This was intended to trap out any water vapour. The storage bulb 3 was filled to about 1 atm. pressure, monitored by the spiral gauge. Stopcock M was closed, the cylinder was disconnected, and trap 1 was warmed and evacuated. Trap 2 was immersed in liquid nitrogen freezing out all the H_2S. Bulb 3 was again evacuated. Bulb to bulb distillation was performed between traps 1 and 2, with the cold side in liquid N_2 and warm side in a dry ice-acetone slush. Usually 4 such bulb-to-bulb distillations were performed. The originally dried H_2S contained a small amount of air as impurity. After bulb-to-bulb distillation, no observable amount of impurity was found by chromatographic analysis, using silical gel and F & M P-0190 columns. Usually only $\frac{1}{2}$ of the H_2S originally filled was left after such bulb-to bulb distillation.

Oxygen

Oxygen was obtained from commercial cylinders manufactured by Airco. It was found to be remarkably pure. The apparatus used for filling oxygen in both storage bulb is shown in fig. 14.

The vacuum system was evacuated and all stopcocks in the sample line closed except L and K. The portable spiral trap was immersed in a dry ice-acetone slosh. The filling system was flushed with oxygen. Trap 1 was immersed in a dry ice-acetone slosh, and trap 2 in liquid nitrogen. Stopcock K was closed and M opened. Liquid oxygen was thus condensed in trap 2. The pressure in the portable trap system was maintained above atmospheric, so that no water vapour could creep into the system. This pressure was indicated by the mercury level in the T tube.

After enough oxygen had been condensed in t rap 2, stopcock M & L were closed, K opened and the cylinder and the portable trap system disconnected. After trap 1 was evacuated, bulb to bulb distillation was performed. Storage bulb 2 was finally filled to about 1 atm., monitored by the spiral gauge. The purified oxygen was analysed by the chromatography with molecular sieves No. 5 and F & M P-0190 columns but no observable impurity was detected.

Carbon Dioxide

"Bone dry" carbon-dioxide was obtained from cylinders manufactured by the Matheson Company. The same filling and

purification techniques was employed as in the case for oxygen. The F & M P-0190 column was used to analyse for purity. No detectable amount of impurity was found.

Sulphur Dioxide

Matheson "anhydrous" sulphur dioxide in cylinder was used for calibration of the chromatographic chart areas. Since a small amount of impurity would not alter the results appreciably, the gas was used without further purification.

Light Filter Solutions

For radiation at 3130 A^{o}, a Hanovia SH 100 lamp in combination with 2 light filter solutions and a glass filter was used. This filter combination was recommended by Kasha[25a] and by Hunt & Davis[25b] to isolate a wave band of about 200 A^{o} width.

a. Potassium Hydrogen Phthalate.

0.500 gm. of A.R. potassium phthalate was dissolved in water and made up to 250 ml. This concentration was used in a 1 cm. thick quartz filter cell. This solution was not stable to photolysis. It was necessary to store the stock in the dark and change the solution in the filter occasionally.

b. Potassium Chromate

0.246 gm. of A.R. potassium Chromate was dissolved in water to make up 500 ml. of solution. This was used in a 1 cm. thick quartz filter cell. This solution was quite

stable to photolysis.

c. Glass Filter

A 2 mm. thick Corning 9863 filter was used in series with the above-mentioned filter solutions.

EXPERIMENTAL PROCEDURE

Experimental Procedure

At the beginning of each experiment, the vacuum system was evacuated so that a dark discharge was obtained in the sample line near the reaction vessel. The lamp and the photometer were allowed to warm up for at least fifteen minutes. The gas chromatographic system was allowed at least thirty minutes for equilibrium to be reached. The furnace was never turned off except for repairs and for removal of the reaction cell. Most of the photochemical experiments were made at 150°C with a few at lower temperatures and a few at 160°C.

1. Photolysis and pyrolysis of H_2S alone.

Transmitted intensity I_o was measured when the reaction cell was empty. The spiral gauge scale reading for an empty sample line was taken. Then with the light shutter open and with all the stopcocks closed except U and W, H_2S was metered into the sample line and the reaction vessel. The timer was immediately made to run. The value of transmitted intensity measured, the reading of the spiral gauge taken and the stopcock X closed. Under the experimental conditions, the gas was warmed up in a negligible amount of time so that the spiral gauge reading corresponded to the actual pressure of the gas in the reaction vessel. Periodic measurements of the intensity were made throughout the experiment.

Experiments on the thermal reaction alone were carried out in a similar manner. In this case, no light was shone

through the reaction cell and no measurement of intensity was necessary.

At the end of the experiment, the recorder for the gas chromatographic system was turned on and trap 3 was immersed in liquid nitrogen. In the meantime, the charcoal column in the chromatographic system was prepared and nitrogen was passed through. This carrier gas was allowed to pass through, one after the other, the by-pass and the gas burette, so that any unwanted helium left over from a previous analysis could be driven away from the bores of the stopcocks. The carrier gas finally was directed to flow through the by-pass and the gas-burette evacuated. All stopcocks were closed except Y, C' and E'. The shutter on the light path was closed. Final readings of time and intensity were made. Stopcock X was opened to allow the condensable gasses to condense in trap 3 and the H_2(product) to pass to the gas burette. C' was then closed, A' and F' opened. The mercury level in the Toeppler pump was allowed to rise. After a few operations of the Toeppler pump, the hydrogen could be exhaustively transferred to the gas burette. By turning stopcocks G' and H' simultaneously, the carrier gas was directed to sweep through the gas burette, carrying the hydrogen into the charcoal column.

When the stopcocks G' and H' were turned, a kick on the recorder chart was registered, marking the starting point. The chart was turned off only after the expected peak or peaks had emerged.

2. Photolysis or pyrolysis of H_2S with CO_2 as an inert gas.

When CO_2 was used as an inert gas, the gas-metering procedure was slightly altered. With all stopcocks closed except P,U, and W, H_2S was admitted by turning the stopcocks. The pressure was measured. The sidearm of the mixing vessel was immersed in liquid nitrogen thus all the H_2S could be frozen here. Stopcock P was closed and the sample line plus the reaction cell were evacuated by opening stopcock O. Then stopcock O was closed again and CO_2 was admitted into the sample line and the reaction cell. Stopcock P was opened so that all the CO_2 in the line and cell could be condensed with the H_2S. Stopcock P was closed again. Liquid nitrogen was removed and the mixture was allowed to warm, while stirring was applied by turning on the magnetic stirrer. In the meantime, stopcock O was opened so that the line and cell could be evacuated. Intensity was measured. Stopcock O was closed. The warmed mixture was admitted to the cell by opening stopcock P. The light shutter was opened, the timer set to run, the pressure measured, and the stopcock X closed. The difference of the two pressures gave the pressure of CO_2.

The analysis part of this experiment followed the same procedure as in part (a) above.

3. Photochemical & Thermal Oxidation of H_2S

The admission of H_2S was the same as described in the previous section. With only stopcocks P,V and W open, H_2S was let into the system by turning stopcocks S. The pressure was recorded. The H_2S was then frozen into the side arm of

the mixing vessel. Stopcock P was closed. Stopcock O was then opened to evacuate the sample line and the reaction cell. W, O were then closed, and P opened. Oxygen was admitted by turning stopcock R. P was next closed. Liquid nitrogen was removed from the side arm of the mixing chamber and the magnetic stirrer turned on. In the mean time, stopcock O was opened to evacuate the sample line and the reaction cell. Initial reading of intensity, I_o , was taken and the light shutter left open. Stopcock O was closed, P opened, The timer was set to run and the total pressure readings gave the pressure of O_2 in the cell. Stopcock W was then closed. Periodic measurements of intensity I_t was made at appropriate intervals.

During the run, the vacuum system other than the reaction cell was constantly pumped. Chromatographic Column F & M P-0190 with helium as carrier gas was prepared. At the end of the experiment, stopcocks V, Y, A', B', D' & F' were closed and C' and E' opened. The light shelter was lowered, reaction time noted, and stopcock X was opened. Y was then opened for about a second to allow the products to flow to the gas burette. Stopcocks C' and E' were closed and G' and H' turned simultaneously, so that the products were swept into the chromatographic column. Trap 3 was immersed in liquid nitrogen and stopcock Y opened. All condensable products and reactants were thus condensed.

After the O_2, H_2S, SO_2 & H_2O had passed through the F & M P-0190 column, the chromatographic system was swept with nitrogen and the charcoal column prepared.

The hydrogen from the reaction cell was Toeppler-pumped into the gas burette by the following sequence of operations. Stopcocks A', B' and D' were closed and then C' opened. C' was closed and A' opened. The mercury level in the Toeppler pump was allowed to rise by letting air into the reservoir through I'. The hydrogen was forced into the gas burette. Repreated operations were performed to transfer the hydrogen practically completely into the gas burette. Stopcock D' was then closed and G' and H' turned simultaneously to allow the hydrogen to be swept into the charcoal column.

The reaction cell and leads were evaluated and the intensity measured.

The procedure for thermal oxidation was the same except that no irradiation was involved.

4. Photochemical and Thermal oxidation of H_2S with CO_2 as an inert gas.

The only difference in procedure from the above section was the admission of CO_2. H_2S was first frozen in the side arm of the mixing vessel and stopcock P was closed. The sample line was evacuated and all stopcocks were closed. CO_2 was admitted to the sample line by turning stopcock Q. The spiral gauge reading was noted. Stopcock P was opened and the CO_2 allowed to greeze in the sidearm of the mixing vessel with the H_2S. Oxygen was admitted in the same way as in the preceeding section. The final pressure of CO_2 in the reaction vessel was calculated from the volume measurements

of the sample line, reaction vessel and mixing vessel, assuming perfect gas behaviour. The pressure of oxygen was found from the difference in total pressure and the pressures of H_2S and CO_2.

The subsequent experimental procedure and analysis were the same as in the preceding section.

RESULTS

Photo-oxidation

Photo-oxidation of hydrogen sulphide was studied at temperatures of 130°C and 150°C. Photolysis of hydrogen sulphide alone gave hydrogen and deposits of sulphur. The products of photolysis of a mixture of hydrogen sulphide and oxygen were SO_2, H_2, and H_2O and sulphur.

Great difficulty was encountered in obtaining reproducible quantitative data. This might arise from a number of reasons.

1. H_2S absorption under experimental conditions was about 1%. Fluctuations in lamp intensities was of this order. Thus it was difficult to measure accurately the light absorbed. This was partially remedied by calculating the light absorbed from a pre-determined absorption coefficient. The absorption of H_2S at 2537 Å and 130°C is shown on fig. 16. It is seen that the Beer-Lambert Law is not strictly followed. For the experimental pressures, however, the portion of the plot is straight and the absorption coefficient for calculating light absorbed has been obtained from this region. Thus

$$\log \frac{I_o}{I_t} = 7.03 \times 10^{-4} P \qquad \text{at } P = 0\text{-}60 \text{ mm.Hg.}$$

2. The extent of the reaction between SO_2 and H_2S was not known. The amount of SO_2 measured could be different from the amount produced.

3. The effect of the surface was not known. Experiments in a packed cell did not reveal any pertinent information. The product in such an experiment was hardly measurable and this could be due to the small free volume of the packed cell. The nature of the surface was also unknown. A clean quartz surface would have a different effect than one which was deposited with finely divided sulphur. However, sulphur was observed only at the colder leads to the cell.

Despite the difficulty in reproducibility, a few observations were definite. The yield of SO_2 and H_2 increased with increase in the initial ratio of $(O_2)/(H_2S)$. This is shown in Table 1. The ratio of quantum yields of SO_2 and of H_2 was about 20 in all photolysis experiments, indicating a chainn reaction in the production of SO_2. This is shown in Table 2.

Photolysis of hydrogen sulphide alone in the packed cell gave hydrogen. The quantity of hydrogen was reduced when oxygen was introduced. The production of SO_2 was not observed after 700 minutes of radiation with a $(O_2)/(H_2S)$ ratio exceeding 2. This might have arisen due to the small amount of reactants photolysed and the low intensity absorbed. However, at this temperature(150^oC) the thermal reaction should have been appreciable. Results of photo-oxidation in the packed cell are shown in Table 3.

Whether in the large cell or the packed cell thermal oxidation was appreciable at 150^oC. It was often difficult to differentiate the quantity of the product due to the thermal reaction or the photo-oxidation. At 130^oC, however, the thermal reaction was negligible. Complete results are shown in the Appendix.

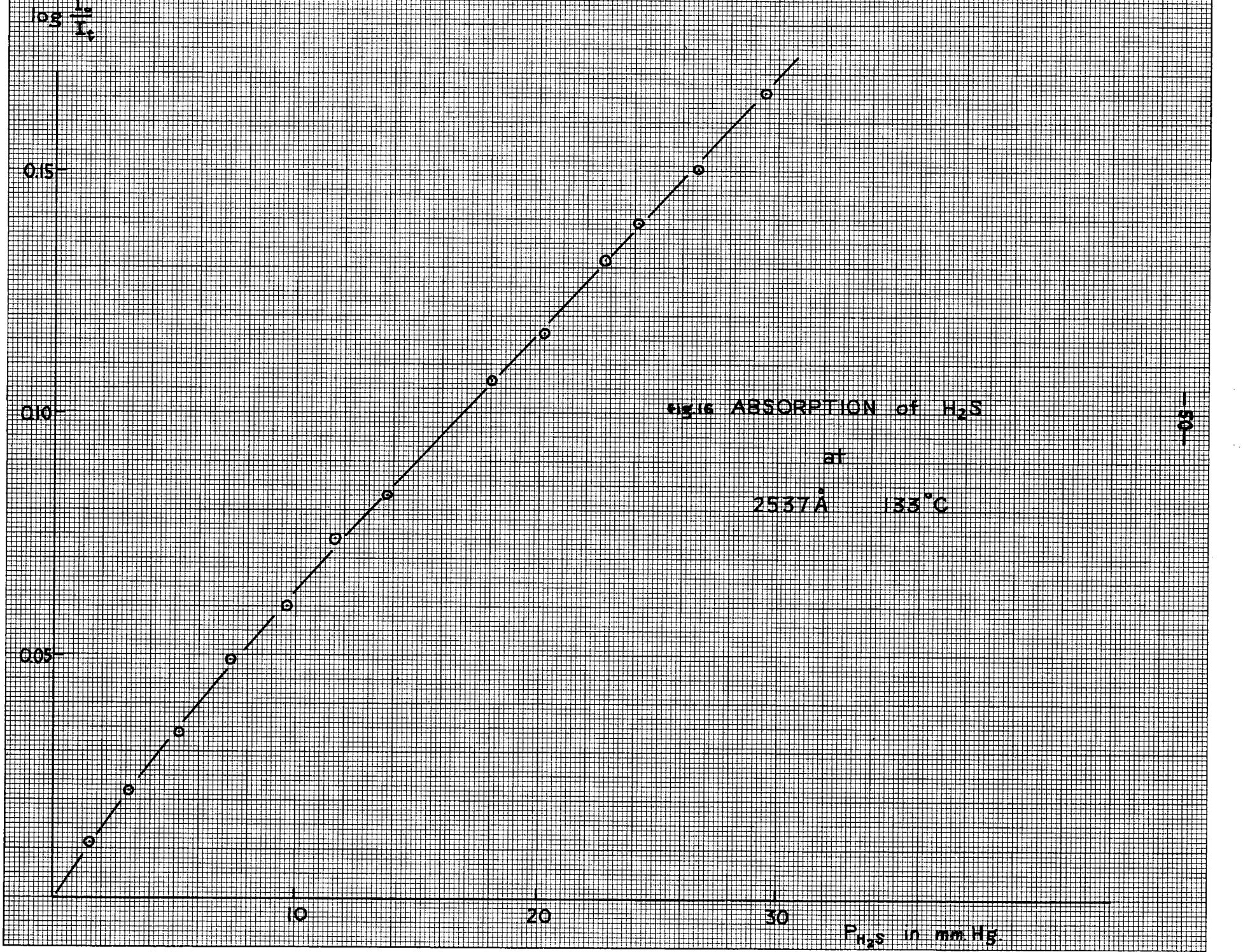

Fig 16 ABSORPTION of H_2S at 2537 Å 133°C

Table 1.

Photooxidation results showing the effect of P_{O_2} : P_{H_2S} ratio on Φ_{SO_2} & Φ_{H_2}

Expt.No.	Temp. °C	Reaction Time min.	I_o	P_{H_2S} mm.	P_{O_2} mm.	P_{CO_2} mm.	P_{O_2}/P_{H_2S}	$\Phi_{SO_2} \times 10^{-3}$	Φ_{H_2}
134	149	75	890	5.5	92.1	-	16.7	7.86	-
132	149	47	930	5.5	90.9	-	16.5	7.15	-
136	152	66	870	5.9	90.4	-	15.5	7.44	-
129	152	45	1080	6.8	96.7	-	14.0	7.70	-
169	149	65	740	6.4	62.5	-	9.78	6.15	-
165	152	244	550	5.9	32.0	-	5.40	3.68	-
159	152	104	770	6.4	25.2	145	3.94	2.05	-
151	154	265	820	5.5	21.6	-	3.92	2.04	-
273	149	150	2010	15.1	40.3		2.67	0.994	55.0
272	149	178	2050	18.5	33.6		1.81	0.348	16.4
271	149	210	2250	15.9	26.0		1.63	0.229	11.4
269	147	203	2090	13.4	12.6		0.94	0.138	7.14
268	147	200	1940	15.4	7.1		0.458	0.046	5.33
322	148	169	3590	18.5	110		6.0	0.188	9.2
324	147	235	3416	16.8	99.4		5.9	0.258	9.8
326	146	415	3270	17.6	96.1		5.5	0.187	7.0
325	145	198	3140	20.6	97.4		4.7	0.068	6.2
323	147	294	3170	23.5	105.8		4.5	0.090	5.6
327	147	149	3054	22.2	91.5		4.1	0.086	5.4

Table 2.

Photo-oxidation results showing consistency of Φ_{SO_2}/Φ_{H_2}

Expt.No.	Temp. °C	Reaction Time min.	I_o	P_{H_2S} mm.	P_{O_2} mm.	P_{O_2}/P_{H_2S}	$\Phi_{SO_2} \times 10^{-3}$	Φ_{H_2}	Φ_{SO_2}/Φ_{H_2}
256	151	243	2340	24.4	44.9	1.84	0.20	0.708	27.4
269	147	203	2090	13.4	12.6	0.94	0.138	7.14	19.4
271	149	210	2250	15.9	26.0	1.63	0.229	11.4	20.1
272	149	178	2050	18.5	33.6	1.81	00.348	16.4	21.2
273	149	150	2010	15.1	40.3	2.67	0.994	55.0	18.6
322	148	169	3580	18.5	110	6.0	0.188	9.2	20.2
323	147	294	3170	23.5	106.8	4.5	0.090	5.6	16.0
324	147	235	3416	16.8	99.4	5.9	0.258	9.8	26.4
325	145	198	3140	20.6	97.4	4.7	0.068	6.2	11.5
326	146	415	3270	17.6	96.1	5.5	0.187	7	23.6
327	147	149	3054	22.2	91.5	4.1	0.086	5.4	16.1
263	148	175	2000	15.5	44.5	2.87	0.787	31.4	25.1
266	148	132	1360	14.3	47.0	3.29	1.14	53.1	21.5
274	148	123	2100	12.2	47.9	3.93	0/252	9.75	25.8
275	146	120	2020	15.5	39.4	2.54	0.206	13.3	15.5
278	147	112	2060	14.7	38.6	2.62	0.516	28.6	18.1
283	145	135	1670	21.8	59.6	2.73	0.357	15.8	22.6
286	134	121	1640	15.1	68.4	4.53	1.39	52.7	26.4
292	136	123	2400	26.0	76.4	2.94	0.222	10.4	21.3
296	136	120	1520	19.3	65.9	3.41	0.835	32	26.1
307	150	255	297	16.8	178.5	10.6	18.7	804	23.3
315	152	331	880	20.2	114	5.59	1.16	58	19.2
318	147	99	3552	15.1	104	6.9	0.104	4.6	23
328	148	230	3014	20.2	87.3	4.3	0.132	7.2	18.2
329	146.3	190	2862	17.6	82.3	4.7	0.062	2.6	23.0
331	151	211	2930	22.1	75.5	3.4	0.090	5.8	15.3
334	149	178	2827	13.9	73.4	5.3	0.132	6.9	19
336	149	204	3350	14.3	61.7	4.3	0.215	11.8	18.3
343	150	209	3270	24.0	45.3	1.9	0.088	4.6	19
359	161	35	2560	10.9	90.6	8.31	9.98	516	19.3
363	169	34	1700	11.3	83.1	7.32	14.1	710	20.0
338	152	234	3170	19.3	43.6	2.3	0.042	3.5	24
344	151	318	3290	16.8	39.4	2.3	0.072	4.3	16.7

Table 3

Photo-oxidation in packed cell.
Volume = 35.4 c.c. Surface/volume ratio = 4.3 $cm.^{-1}$

Expt.No.	Temp. ^{o}C	Reaction Time min.	I_o Ω	P_{H_2S} mm.	P_{O_2} mm.	P_{O_2}/P_{H_2S}	$\Phi_{SO_2} \times 10^{-3}$	Φ_{H_2}
379	149.3	205	450	7.1	88.2	12.4	0	20.2
380	150.2	322	620	21.0	92.0	4.38	0	6.2
381	149.0	182	655	11.3	77.6	6.87	0	0
382	154.1	433	630	12.6	78.5	6.23	0	0
383	153.1	641	600	18.9	68.1	3.61	0	0
384	151.0	650	650	10.9	84.8	7.78	0	31.2
385	150.6	645	605	10.9	86.5	7.94	0	22.8
388	150.6	612	650	28.2	0	-	-	8.8
389	152.2	670	660	20.2	126	6.25	0	1.4
390	152.2	575	640	15.1	135.6	8.98	0	2.2
391	152.2	406	650	25.2	0	-	-	9.2
392	152	589	610	24.8	73.9	2.98	0	3.4
393	149.5	559	-	18.9	125.1	6.62	0	0

Thermal Oxidation

Thermal oxidation of hydrogen sulphide was studied at temperatures of 160°, 170°, 190°, 210°, 225°, 240° and 260°C. Products were SO_2, H_2O and sulphur. No hydrogen was found. About 3×10^{-8} gm.mole of hydrogen could be detected on the charcoal column. The amount of SO_2 usually produced was of the order of 5×10^{-6} gm.mole. The yield of SO_2 increased drastically with slight increase in $(O_2)/(H_2S)$ ratio. Under certain conditions at 260°C, 19 mm. of hydrogen sulphide and 26 mm. of oxygen (ratio = 1.33) led to a small explosion with a light emission about 5 seconds after introduction of the mixture into the reaction vessel. Increased pressure, with the ratio of $(O_2)/(H_2S)$ kept constant also increased the yield, as shown on Table 4 and fig. 17.

Runs were made (a)holding the oxygen pressure constant and (b)holding the hydrogen sulphide pressure constant. Initial rates were calculated at less than 10% completion. log(initial rate) was plot against $\log(H_2S)$ or $\log(O_2)$ as the case might be. The order of reaction was calculated from the slope. The plot showing runs with (O_2) held constant at 258.5°C is shown in Table 5 and fig. 18. It is seen that the order with respect to (H_2S) varies with (H_2S) from 1 to 0 to -1 and again to 0. The plots for runs with (H_2S) held constant at seven temperatures are shown in Tables 6-12 and figs. 19-25. It is obvious that the order with respect to (O_2) is 3. Overall results could be expressed as

$$\text{Rate} = k(H_2S)^{-1 \rightarrow +1}(O_2)^3.$$

The slopes and intercepts of these lines were calculated by the least squares method. The initial rates for (H_2S)

$= 9.75 \times 10^{-5}$ gm. mole in the reaction cell and $(O_2) = 1.00 \times 10^{-4}$ gm. mole for seven temperatures were calculated and plot against 1/T. This plot, shown on Table 13 and fig. 26, turned out to be a smooth curve, but the closest least squares line gave and overall activation energy of 21.2±2k.cal./mole.

The effect of inert gas(CO_2) at 260°C was studied. The effect of CO_2 up to 3 times the total pressure of hydrogen sulphide and oxygen together was not appreciable. Complete results are shown in the Appendix.

Table 4.

Thermal Oxidation - Effect of total pressure - 256.6°C.

Expt.No.	Temp. °C.	Reaction Time min.	P_{H_2S} mm.	P_{O_2} mm.	P_{total} mm.	P_{O_2}/P_{H_2S}	Initial Rate x10^6 gm.mole/min.
509	258.1	2.0	15.5	13.9	29.4	0.892	0.85
519	257.9	2.1	21.0	18.1	39.1	0.860	2.71
520	257.0	1.9	15.1	10.5	25.6	0.694	0.474
523	255.6	2.8	21.4	18.1	39.5	0.843	2.16
524	256.9	2.5	22.2	19.7	41.9	0.887	3.68
525	257.4	2.4	19.7	16.8	36.5	0.851	2.10
526	258.3	2.2	31.9	26.9	58.8	0.842	4.78
529	256.3	4.6	50.0	44.1	94.1	0.883	5.33
530	255.8	1.9	33.6	29.0	62.6	0.862	6.0
531	256.7	2.4	45.4	32.3	77.7	0.713	5.91
510	256.9	2.4	25.6	24.8	50.4	0.967	5.88
514	254.0	4.8	24.4	23.1	47.5	0.948	2.56
517	259.0	2.3	23.1	22.2	45.3	0.964	3.04
527	255.7	3.2	26.4	24.8	51.2	0.936	3.42
528	254.4	3.3	38.2	37.0	75.2	0.967	6.18
513	254.8	3.1	19.7	21.8	41.5	1.11	3.97
515	255.2	1.8	27;3	28.1	55.4	1.03	10.4
516	259.0	2.3	23.1	25.2	48.3	1.09	6.65
522	255.6	2.3	22.7	23.5	46.2	1.04	6.48

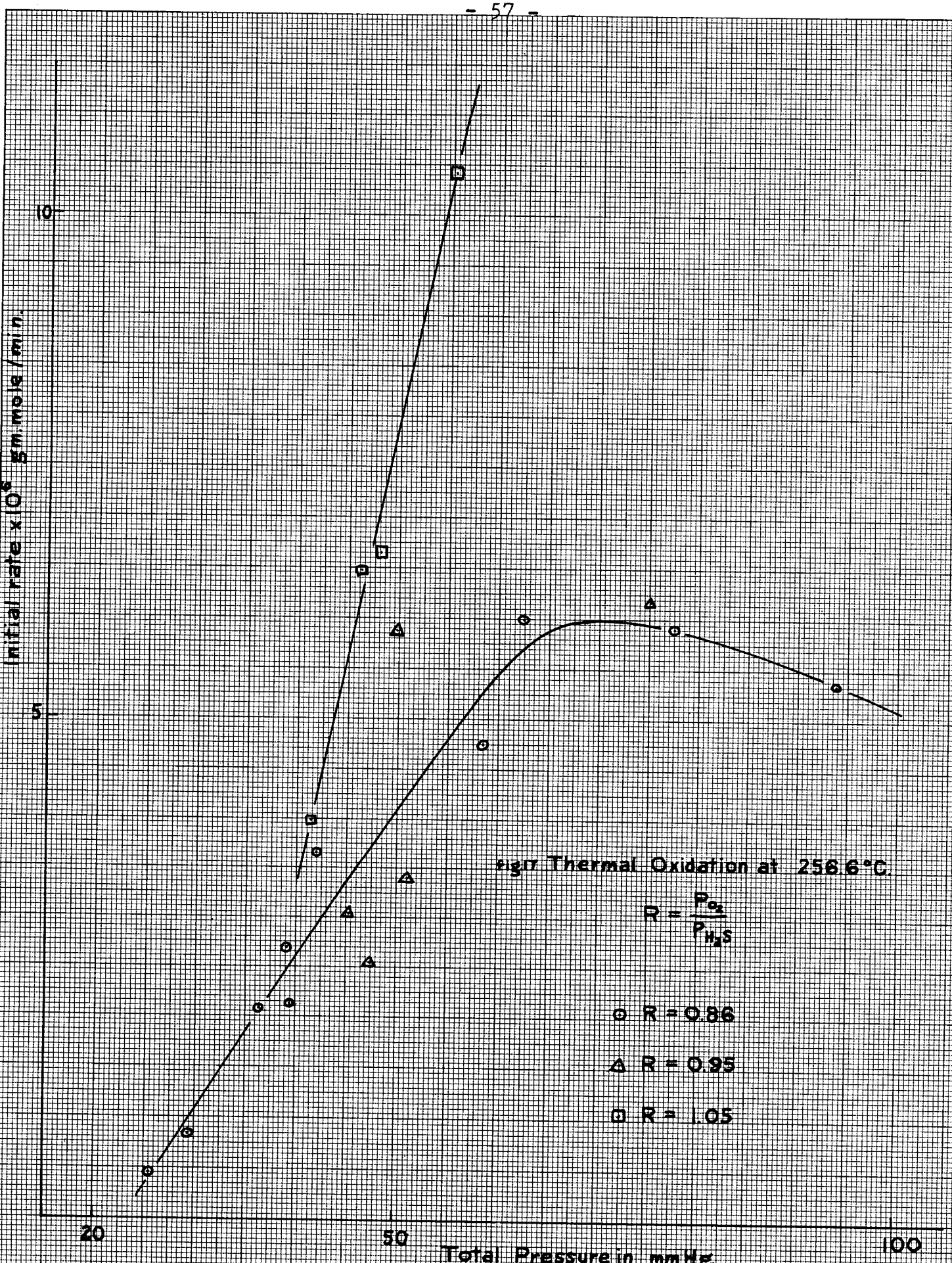

Fig 17 Thermal Oxidation at 256.6 °C.

Table 5.

Thermal Oxidation at 258.3°C.
$(O_2) = 1.26 \times 10^{-4}$ gm. mole in the reaction cell.

$r = \Delta(SO_2)/\Delta t$ = initial rate in gm.mole/min.

Expt. No.	Temp. °C	Reaction Time min.	$\log(H_2S)$	log r
The straight portion of the plot:				
474	258.5	3.8	-4.788	-5.628
477	256.3	3.8	-4.450	-5.306
482	255.4	1.4	-4.383	-5.025
483	256.1	1.8	-4.168	-4.890
484	257.1	1.4	-4.131	-4.833
504	259.9	2.3	-4.090	-4.754
505	260.0	2.0	-4.206	-4.827
506	260.0	2.1	-4.312	-4.992
507	260.0	2.5	-4.432	-5.188
Thus $\log r = 1.27 \times \log(H_2S) + 0.44$				
The curved portion of the plot:				
485	256.3	2.0	-3.998	-4.896
486	255.1	1.7	-3.979	-4.862
487	253.5	1.7	-3.921	-4.857
488	258.1	2.2	-5.820	-5.138
489	258.9	1.7	-3.697	-5.134
490	259.0	3.1	-3.590	-5.336
491	259.6	3.2	-3.527	-5.430
492	254.4	2.6	-3.434	-5.484
493	260.6	3.3	-3.340	-5.545
495	256.1	3.7	-3.270	-5.579
496	263.1	3.1	-3.234	-5.582
497	263.0	2.2	-3.955	-4.961
498	258.7	2.1	-3.852	-5.107
499	259.5	2.0	-3.961	-4.911
500	260.2	1.5	-3.821	-4.904
501	260.7	1.7	-3.918	-4.827
502	257.6	2.1	-3.857	-5.084
503	257.6	2.5	-3.772	-5.258

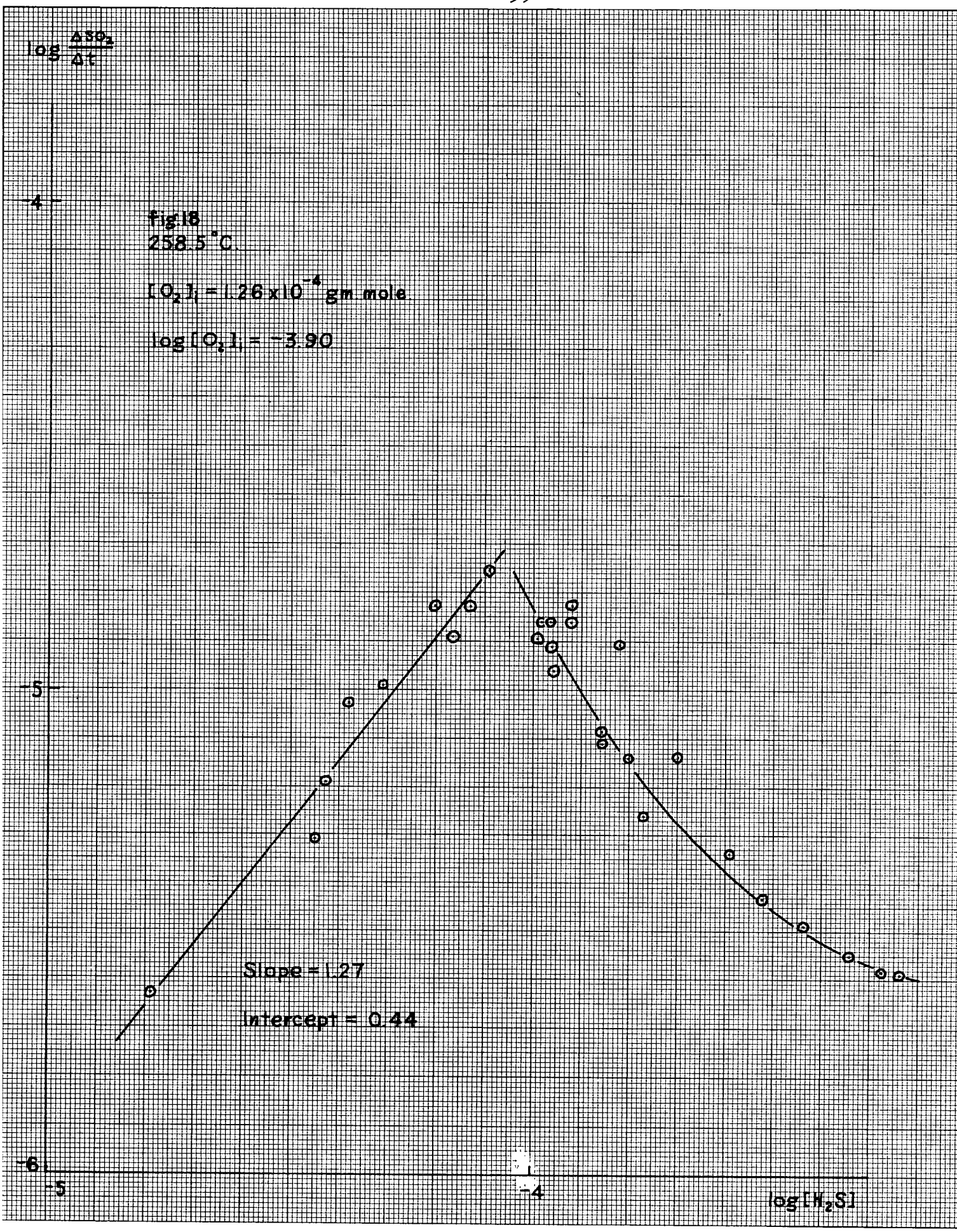
log Δso₂/Δt
-4
-5
-6
-5
-4
log [H₂S]
fig 18
25 8.5 °C.
[O₂]ᵢ = 1.26 x 10⁻⁴ gm mole
log [O₂]ᵢ = -3.90
Slope = 1.27
Intercept = 0.44

Table 6.

Thermal Oxidation at 162.0°C.

$(H_2S) = 9.59 \times 10^{-5}$ gm.mole in reaction cell

$r = \Delta(SO_2)/\Delta t$ = initial rate in gm.mole/min.

Expt. No.	Temp. °C	Reaction Time min.	$\log(O_2)$	log r
573	162.4	55.1	-4.627	-9.750
574	162.5	52.0	-4.398	-9.424
575	162.1	103.9	-4.206	-7.864
576	161.5	93.3	-4.074	-7.444
578	161.5	58.5	-3.818	-6.714
579	163.4	33.3	-3.629	-6.179
581	161.8	84.6	-3.950	-7.125
582	160.9	50.8	-3.772	-6.684
583	161.4	24.0	-3.618	-6.578
584	161.2	19.5	-3.556	-6.218

Thus $\log r = 2.90 \times \log(O_2) + 4.31$

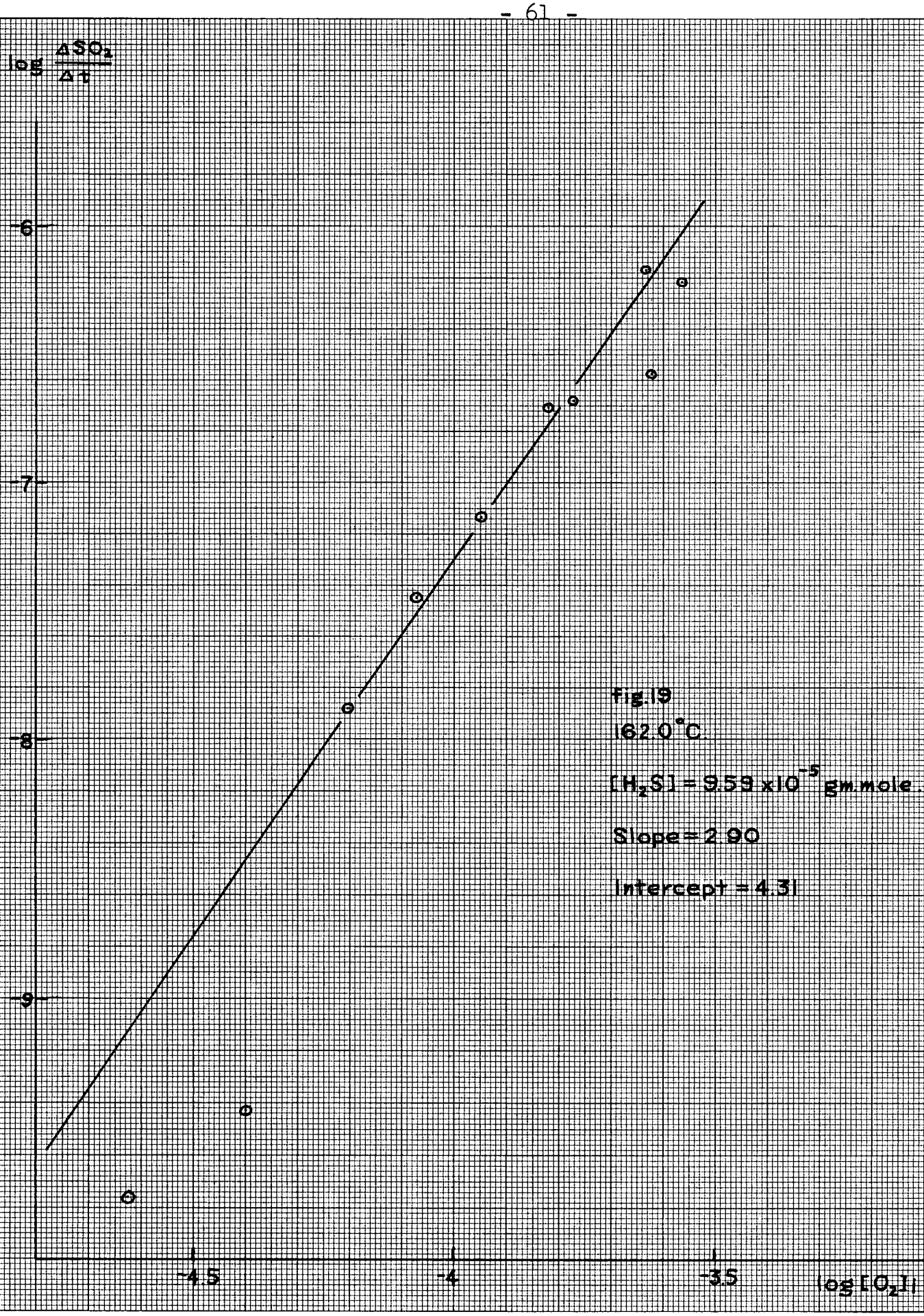

Fig.19
162.0 °C.
$[H_2S] = 9.59 \times 10^{-5}$ gm.mole.
Slope = 2.90
Intercept = 4.31

Table 7.

Thermal Oxidation at 171.4°C.

$(H_2S) = 9.30 \times 10^{-5}$ gm.mole in reaction cell

$r = \Delta(SO_2)/\Delta t$ = initial rate in gm.mole/min.

Expt. No.	Temp. °C	Reaction Time min.	$\log(O_2)$	log r
585	172.0	137	-4.368	-7.666
586	169.6	73.8	-3.998	-6.871
587	170.7	36.2	-3.745	-6.044
588	171.6	37.8	-3.836	-6.256
589	170.7	67.0	-4.114	-7.242
590	172.6	27.8	-3.631	-5.851
591	172.6	18.0	-3.640	-5.902

Thus $\log r = 2.96 \times \log(O_2) + 4.91$

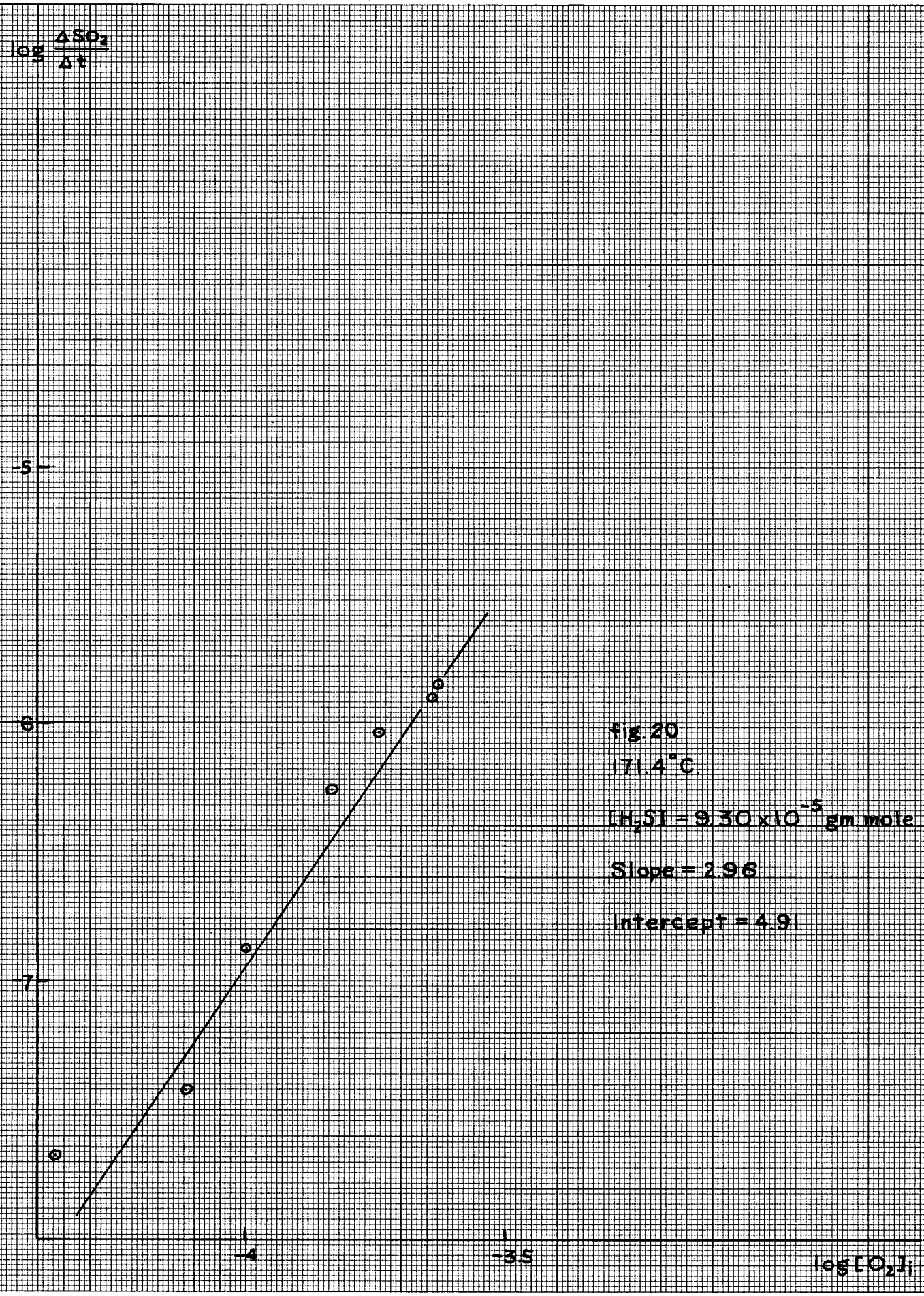

Fig. 20

171.4°C.

$[H_2S] = 9.30 \times 10^{-5}$ gm mole

Slope = 2.96

Intercept = 4.91

Table 8.

Thermal Oxidation at 191.0°C

$(H_2S) = 9.24 \times 10^{-5}$ gm.mole in reaction cell

$r = \Delta(SO_2)/\Delta t$ = initial rate in gm.mole/min.

Expt. No.	Temp. °C	Reaction Time min.	$\log(O_2)$	log r
566	189.6	35.6	-4.830	-8.854
567	189.6	34.4	-4.528	-7.893
568	190.6	29.5	-4.228	-6.938
569	191.8	11.1	-4.004	-6.180
570	191.8	9.1	-3.955	-6.016
571	191.8	4.1	-3.757	-5.682
572	192.3	4.1	-3.605	-5.296

Thus $\log r = 2.96 \times \log(O_2) + 5.55$

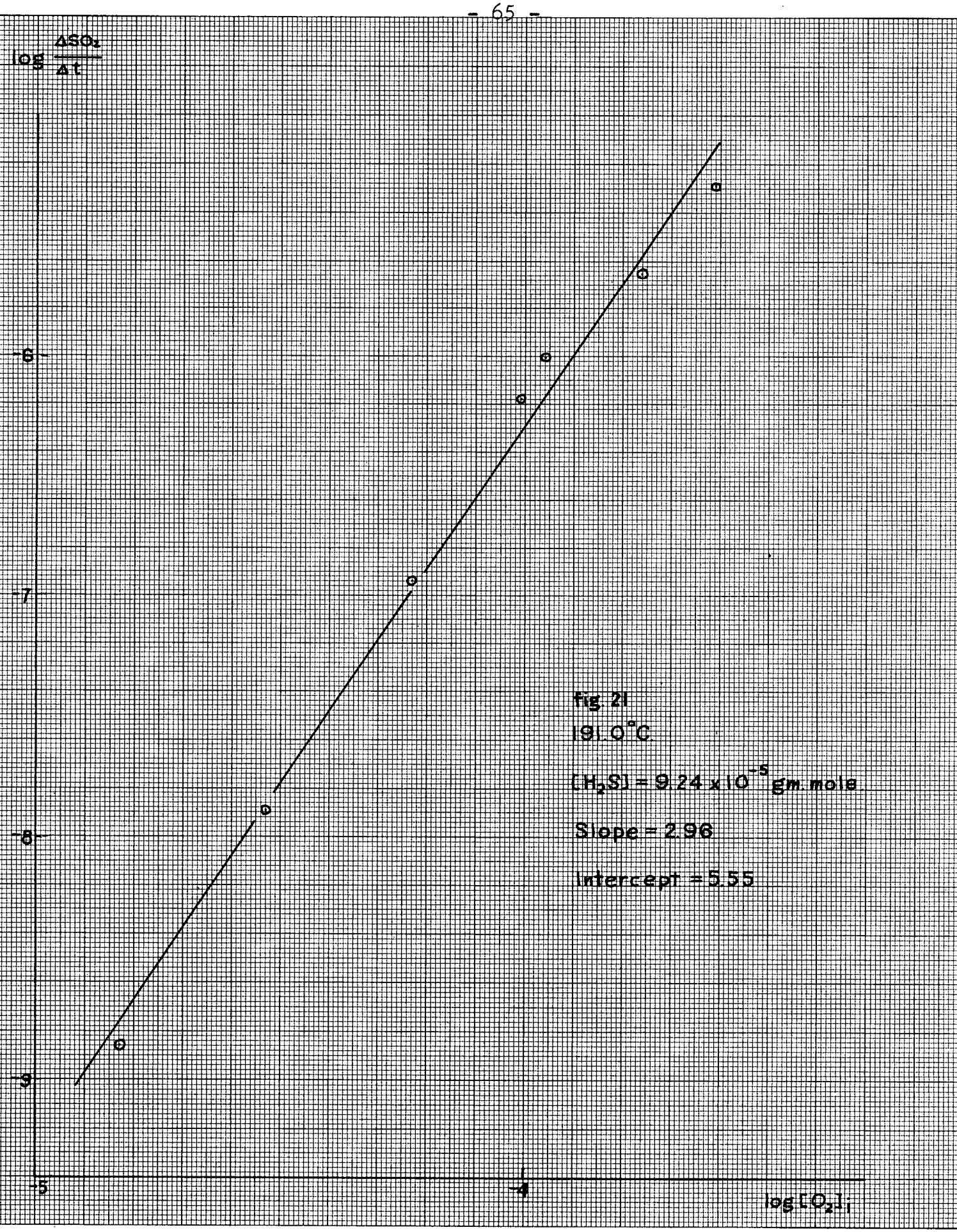

fig. 21

191.0°C

$[H_2S] = 9.24 \times 10^{-5}$ gm. mole

Slope = 2.96

Intercept = 5.55

Table 9.

Thermal Oxidation at 209.5°C.

$(H_2S) = 9.80 \times 10^{-5}$ gm.mole in reaction cell

$r = \Delta(SO_2)/\Delta t$ = initial rate in gm.mole/min.

Expt. No.	Temp. °C	Reaction Time min.	$\log(O_2)$	log r
556	211.2	29.7	-5.050	-8.775
557	210.3	37.7	-4.575	-7.424
558	208.3	17.7	-4.383	-6.995
559	209.6	10.3	-4.206	-6.428
560	207.6	10.1	-4.217	-6.460
561	209.6	2.8	-3.900	-5.430
562	208.2	4.0	-4.074	-5.854
563	210.8	2.0	-3.794	-5.168
564	212.6	2.2	-3.772	-5.150
565	209.2	2.2	-3.733	-5.078

Thus $\log r = 2.89 \times \log(O_2) + 5.78$

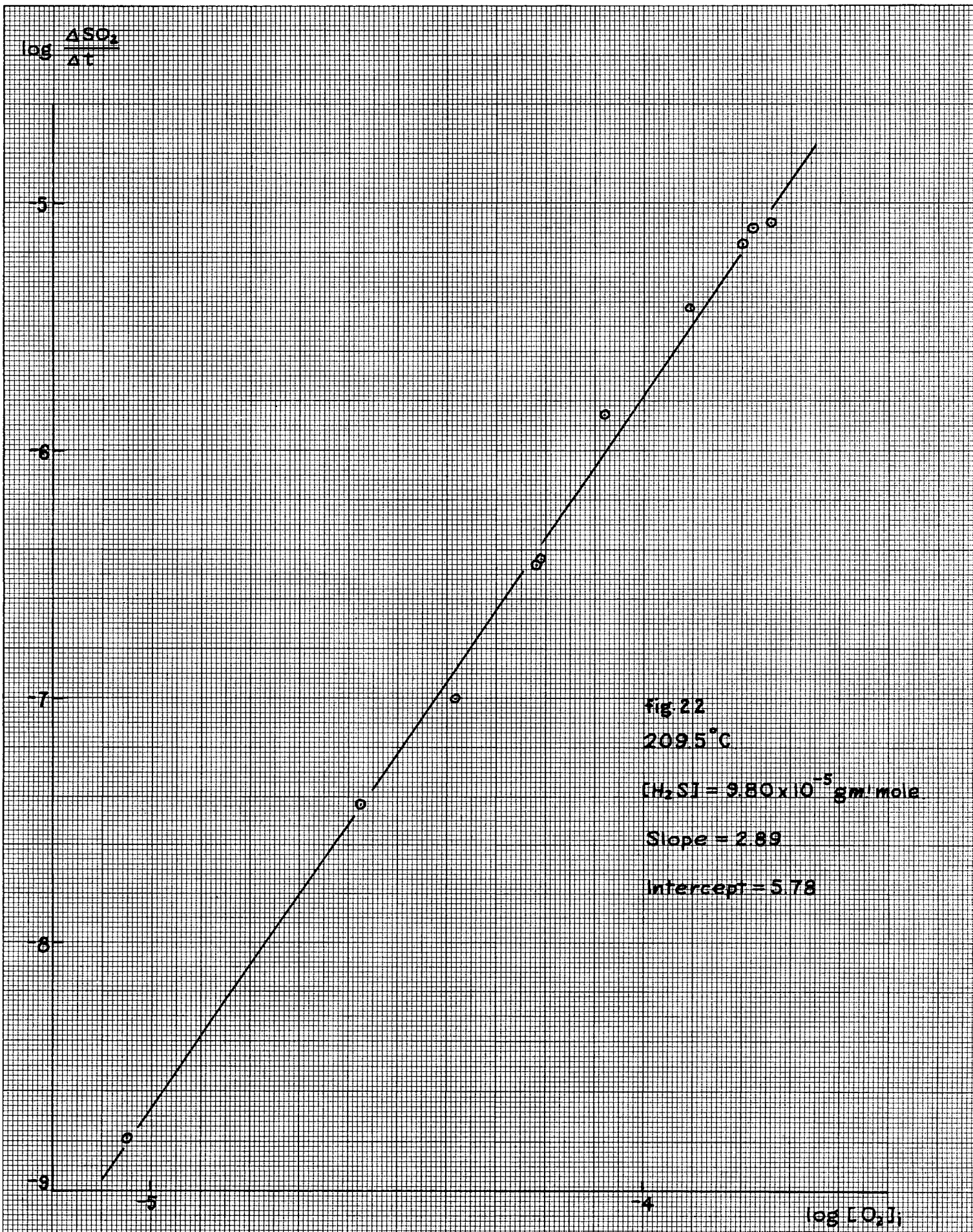

Fig. 22

209.5°C.

$[H_2S] = 9.80 \times 10^{-5}$ gm. mole

Slope = 2.89

Intercept = 5.78

Table 10.

Thermal Oxidation at 225.0°C.
(H_2S) = 9.91×10^{-5} gm.mole in reaction cell
$r = \Delta(SO_2)/\Delta t$ = initial rate in gm.mole/min.

Expt. No.	Temp. °C	Reaction Time min.	$\log(O_2)$	log r
546	225.3	20.8	-4.788	-7.700
547	224.5	24.5	-4.684	-7.487
548	223.7	13.6	-4.338	-6.678
549	223.3	10.0	-4.250	-6.444
550	227.8	4.2	-4.097	-5.802
551	227.1	3.9	-3.921	-5.212
552	225.6	3.5	-3.838	-4.921
553	224.1	2.6	-3.782	-4.936
554	224.8	1.4	-3.740	-4.673
555	224.1	1.7	-3.684	-4.660

Thus $\log r = 2.91 \times \log(O_2) + 6.15$

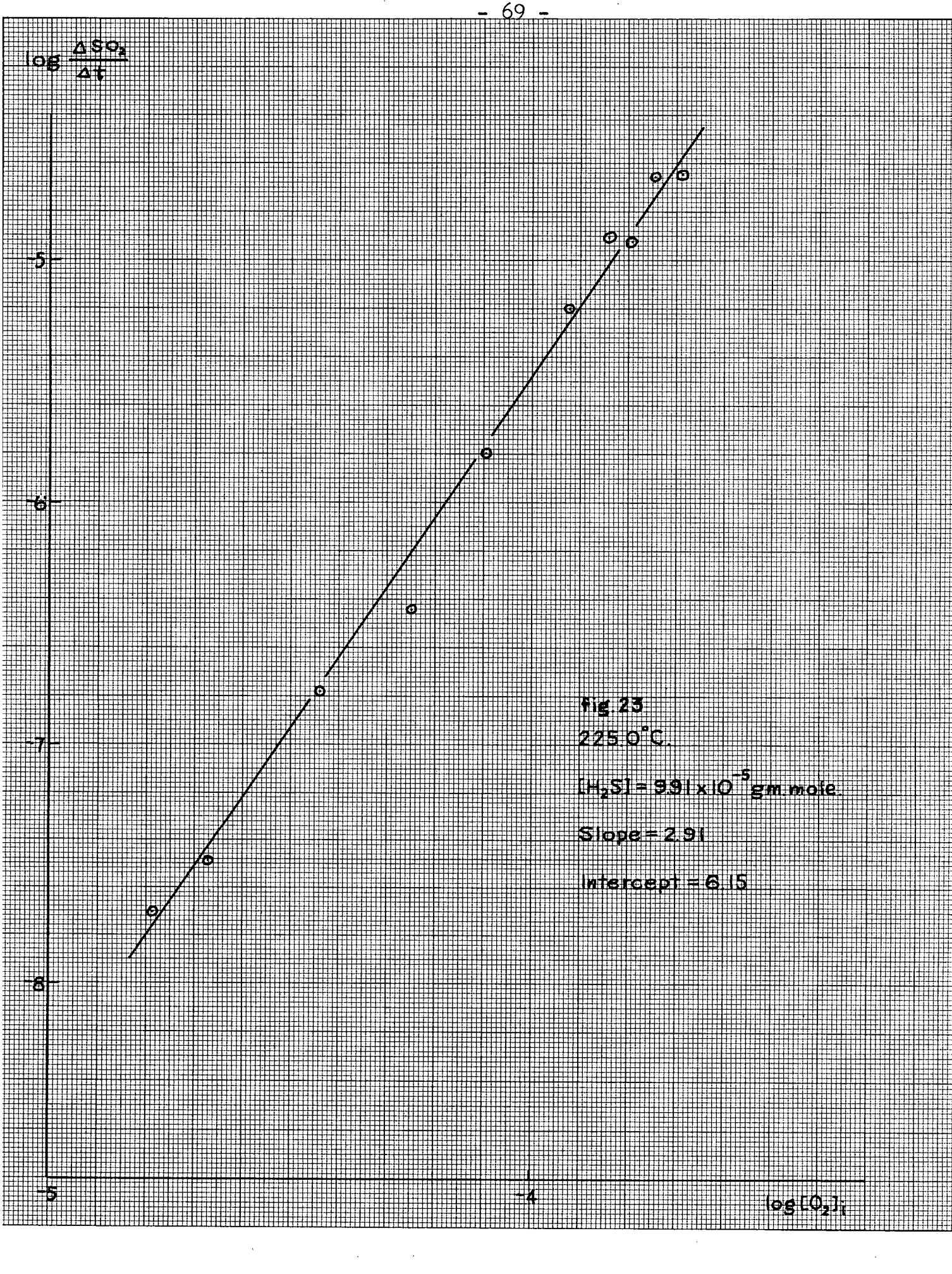

Fig. 23

225.0°C.

$[H_2S] = 9.91 \times 10^{-5}$ gm. mole.

Slope = 2.91

Intercept = 6.15

Table 11.

Thermal Oxidation at 240.5°C.

$(H_2S) = 9.24 \times 10^{-5}$ gm.mole in reaction cell.

$r = \Delta(SO_2)/\Delta t$ = initial rate in gm.mole/min.

Expt. No.	Temp. °C	Reaction Time min.	$\log(O_2)$	log r
537	243.6	4.6	-4.830	-7.622
538	243.5	21.9	-4.684	-7.396
539	240.9	10.9	-4.432	-6.767
540	240.6	3.8	-4.186	-5.917
541	239.3	10.4	-4.368	-6.616
542	239.0	2.6	-4.031	-5.385
543	239.8	1.4	-3.951	-4.962
544	239.8	1.7	-3.838	-4.807
545	239.1	1.2	-3.660	-4.514

Thus $\log r = 2.93 \times \log(O_2) + 6.34$

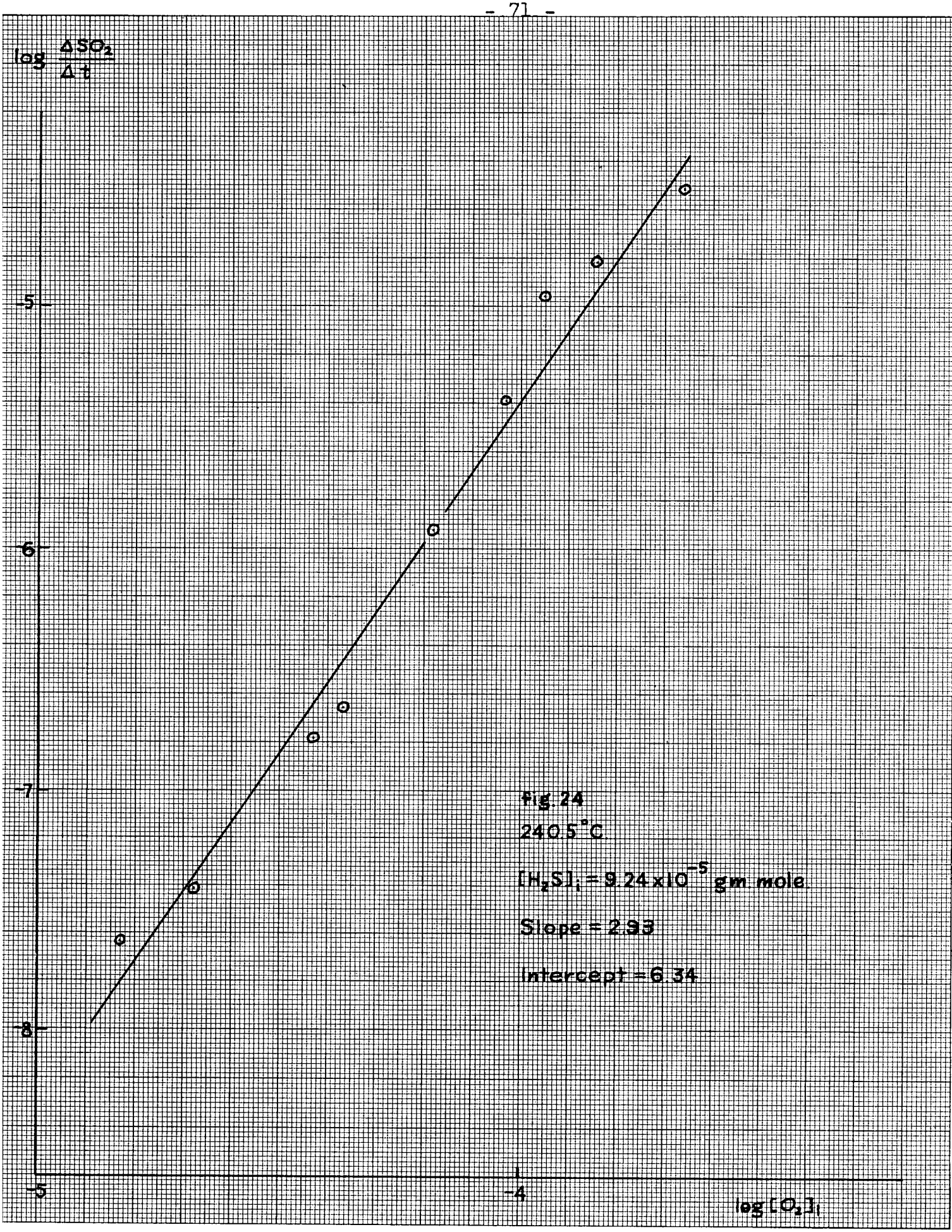

Fig. 24

240.5°C.

$[H_2S]_i = 9.24 \times 10^{-5}$ gm. mole.

Slope = 2.93

Intercept = 6.34

Table 12.

Thermal Oxidation at 258.5°C.

$(H_2S) = 1.12 \times 10^{-4}$ gm.mole in reaction cell

$r = \Delta(SO_2)/\Delta t$ = initial rate in gm.mole/min.

Expt. No.	Temp. °C.	Reaction Time min.	$\log(O_2)$	log r
455	259.0	0.2	-4.114	-5.784
447	258.0	4.5	-4.052	-5.674
442	260.5	4.6	-3.961	-5.405
434	262.3	3.0	-3.917	-5.384
431	260.9	6.1	-3.961	-5.468
430	260.9	5.1	-3.979	-5.408
448	258.0	4.1	-3.817	-4.984
449	258.0	3.9	-3.921	-5.296
450	258.0	6.4	-3.830	-5.178
451	258.0	4.1	-3.927	-5.186
453	256.3	4.4	-3.666	-4.869
454	257.7	5.1	-3.740	-4.952
455a	256.1	1.8	-3.678	-4.536
456	256.2	2.0	-3.733	-4.624
457	257.0	3.8	-3.827	-4.980
458	259.2	4.0	-3.876	-5.223
459	257.9	4.1	-3.998	-5.457
460	257.9	5.1	-4.097	-5.830
462	255.9	4.6	-4.114	-5.820
463	257.7	4.4	-4.166	-5.905
464	256.9	4.2	-4.298	-6.203
465	259.7	8.2	-4.383	-6.488
466	260.9	12.6	-4.654	-7.146
467	259.9	20.5	-4.928	-7.900

Thus $\log r = 2.56 \times \log(O_2) + 4.72$

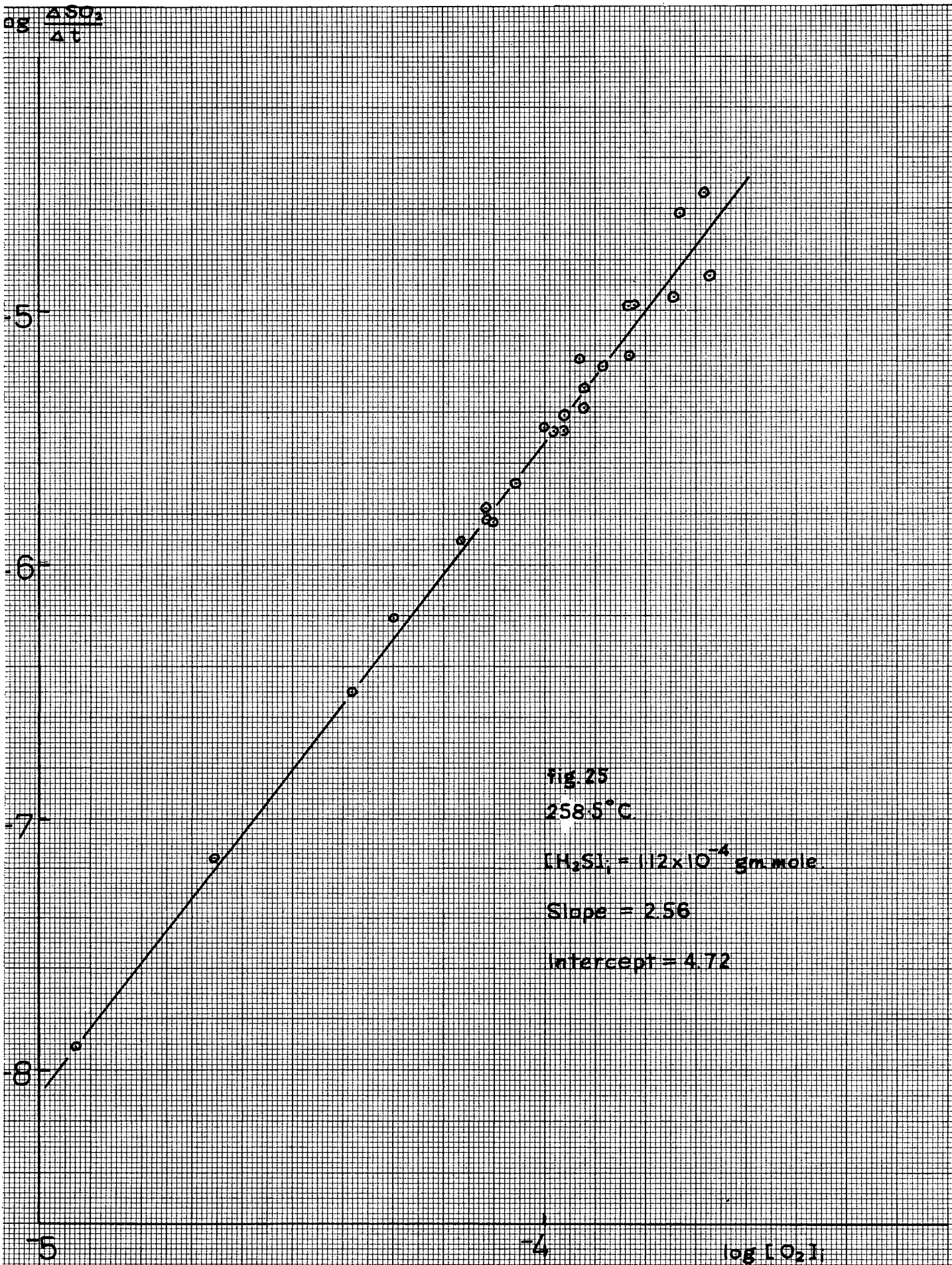

fig. 25

258.5°C.

$[H_2S]_i = 1.12 \times 10^{-4}$ gm. mole.

Slope = 2.56

Intercept = 4.72

Table 13.

Thermal Oxidation - Dependence of initial rate on Temperature.

$r = \Delta(SO_2)/\Delta t$ = initial rate when

$(H_2S) = 9.75 \times 10^{-5}$ gm.mole in reaction cell

$(O_2) = 1.00 \times 10^{-4}$ gm.mole in reaction cell.

Temp. °C.	$1/T \times 10^3$	log r
258.5	1.881	-5.52
240.5	1.947	-5.38
225.0	2.007	-5.49
209.5	2.072	-5.78
191.0	2.154	-6.29
171.4	2.249	-6.93
162.0	2.298	-7.29

Thus $\log r = -4.66 \times 10^3/T + 3.62$

Therefore, overall activation energy = 21.2±1k.cal./mole.

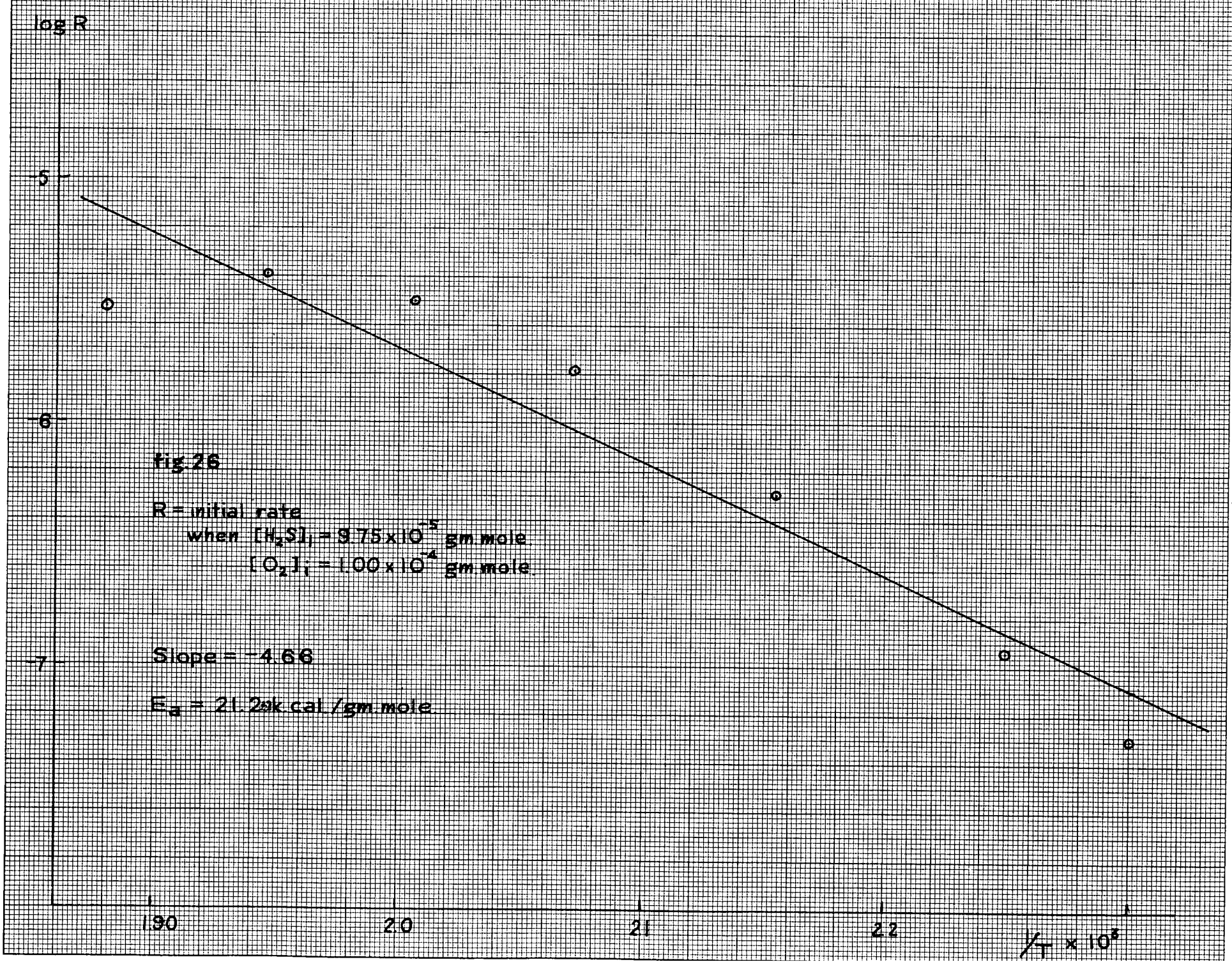

fig. 26

R = initial rate
when $[H_2S]_i = 9.75 \times 10^{-5}$ gm mole
$[O_2]_i = 1.00 \times 10^{-4}$ gm mole

Slope = −4.66

E_a = 21.2 k.cal./gm mole.

D I S C U S S I O N

Photo-oxidation

In the photo-oxidation, difficulty in obtaining reproducibility made quantitative measurements of little value. The possible explanation for this difficulty have been described earlier under "Results". It should be expected that all the factors mentioned played a part. In all previous work the fact that hydrogen sulphide reacted with sulphur dioxide to deposit sulphur was neglected. This could have been the most important factor in affecting reproducibility, since when any sulphur was deposited, a new surface was formed on the walls of the vessel. There was no evidence that the vessel could be "seasoned".

S_2O_2 was not found at all by gas chromatography. It should be expected that under the chromatographic conditions, the S_2O_2 would have decomposed before reaching the detector.

The fact that H_2 was found in the photolysis of hydrogen sulphide alone agreed with the generally accepted initiation steps:

$$H_2S \longrightarrow SH + H$$

$$H + H_2S \longrightarrow H_2 + SH$$

In the presence of oxygen, these were the initiation steps as well.

Darwent and his co-workers[17, 18] did not measure sulphur dioxide as a product and their conclusions could not be complete without considering the sulphur dioxide production. In the present work, the quantum yield of hydrogen increased with the addition of oxygen and with the increase in $(O_2)/(H_2S)$ ratio. This could be due to oxygen inhibiting the terminating reaction:

$$H + SH \longrightarrow H_2S^*$$

The increase in quantum yield of sulphur dioxide could be due

to the same effect. More important, however, could be oxygen as a third body preventing collision of hydrogen sulphide with sulphur dioxide in the overall reaction:

$$2H_2S + SO_2 \longrightarrow 3S + 2H_2O$$

Similar results were obtained by Thompson and Kelland[28] but no plausible explanations were made. The same results were not observed by both Darwent and his co-workers[17,18] and Norrish and his collaborators[15,16].

The common ratio of $I_{SO_2}/I_{H_2} \sim 20$ indicates that sulphur dioxide must be produced by a complicated chain reaction. It is likely the sulphur dioxide is produced in more than one reaction. This observation was not made by either Darwent and his co-workers[17,18] nor by Norrish and his collaborators[15,16], since they did not measure the quantum yields of both sulphur dioxide and hydrogen.

The fact that sulphur dioxide has not been found in the photo-oxidation in the packed cell indicates that termination steps in the chain reaction producing sulphur dioxide must be heterogeneous. The production of hydrogen was not inhibited by the increase in surface area. Any proposed mechanism must be in agreement with this fact.

Thermal Oxidation

In the thermal oxidation, it was significant that hydrogen was not found, indicating that

$$H_2S + M \longrightarrow H + SH + M$$

was not the initiation step, as postulated by Norrish and his co-workers[15]. A more reasonable suggestion would be

$$H_2S + O_2 \longrightarrow SH + HO_2$$

with the HO_2 radical disappearing subsequently at the wall.

The variations in the order for (H_2S) with H_2S pressure could be explained in the following way. The first part of the plot with order = 1 was probably the genuine $H_2S + O_2$ reaction. In the region where order = -1, a retardation by H_2S was indicated and this was probably due to the reaction

$$2H_2S + SO_2 \longrightarrow 3S + 2H_2O$$

In the region where the rate is independent of H_2S pressure, the hydrogen sulphide was in such a large excess that (H_2S) could be considered as constant. S_2O_2 was not found as in the case of photo-oxidation.

It is difficult to comprehend the rate being dependent on the third order with respect to oxygen. A complicated chain reaction must take place. To explain the overall rate expression of

$$\text{Rate} = k(H_2S)^{-1 \rightarrow +1}(O_2)^3$$

the following mechanism is postulated:

Initiation:	$H_2S + O_2 \longrightarrow SH + HO_2$		(1)
Chain propagation:	$SH + O_2 \longrightarrow SO + HO$		(2)
	$HO + H_2S \longrightarrow H_2O + SH$		(3)
Chain branching:	$SO + O_2 \longrightarrow SO_2 + O$		(4)
	$O + H_2S \longrightarrow SH + HO$		(5)
Termination:	$SO + O \longrightarrow SO_2^* \xrightarrow{M} SO_2$		(6)
	$SO + SO \rightleftharpoons S_2O_2$		(7)
	$S_2O_2 + O_2 \longrightarrow 2SO_2$		(8)
	$HO \longrightarrow$ wall		(9)
	$O \longrightarrow$ wall		(10)
	$SH \longrightarrow$ wall		(11)
	$HO_2 \longrightarrow$ wall		(12)

By stationary state considerations,

For $\frac{d(SH)}{dt} = 0$, $k_1(H_2S)(O_2) - k_2(O_2)(SH) + k_3(H_2S)(HO) + k_5(H_2S)(O) - k_{11}(W)(SH) = 0.$

For $\frac{d(SO)}{dt} = 0$, $k_2(O_2)(SH) - kk_4(O_2)(SO) - k_6(SO)(O) - k_{10}(W)(O) - k_7(SO)^2 + k_{-7}(S_2O_2) = 0.$

For $\frac{d(HO)}{dt} = 0$, $k_2(O_2)(SH) + k_3(H_2S)(HO) - k_9(W)(HO) + k_5(H_2S)(O) = 0$

For $\frac{d(O)}{dt} = 0$, $k_4(O_2)(SO) - k_5(H_2S)(O) - k_6(SO)(O) - k_{10}(W)(O) = 0.$

For $\frac{d(S_2O_2)}{dt} = 0$, $k_7(SO)^2 - k_{-7}(S_2O_2) - k_8(O_2)(S_2O_2) = 0.$

An expression for (SO) can be obtained from the above equations using the following assumptions for simplifications

$$k_9(W) \ll k_3(H_2S)$$
$$k_6(SO) \ll k_5(H_2S)$$
$$k_{10}(W) \ll k_5(H_2S)$$

then

$$a(SO)^2 + b(SO) + c = 0$$

where

$$a = \frac{k_{11}(W)\{k_7[k_{-7} + k_8(O_2)] + k_2k_4k_6[k_{-7} + k_8(O_2)](O_2) + k_5k_7k_{-7}(H_2S)\}}{k\,k\,[k_{-7} + k_8(O_2)](O_2)}$$

$$b = -k_4[k_5k_7(H_2S) + k_4](O_2) + \frac{k_4k_{11}}{k_2}(W) + \frac{k_4k_{10}k_{11}(W)}{k_5(H_2S)}$$

$$c = k_1(H_2S)(O_2)$$

The solution is

$$(SO) = \frac{-b \pm \sqrt{b^2 - 4ac}}{2a}$$

It is clear that the solution cannot be explicitly expressed, but will have the form

$$(SO) = a_1(O_2)^2 + a_2(O_2) + a_3$$

where a_1, a_2, a_3..... are coefficients of terms of (O_2).

Therefore,

$$(O) = \frac{k_4(O_2)}{k_5(H_2S)}\ (SO)$$

$$= a_4(O_2)^3 + a_5(O_2)^2 + a_6(O_2) + a_7$$

$$(S_2O_2) = \frac{k_7(SO)^2}{k_{-7} + k_8(O_2)}$$

$$= a_8(O_2)^3 + a_9(O_2)^2 + a_{10}(O_2) + a_{11}$$

Thus from reaction (4),

$$\text{Rate} = \frac{d(SO_2)}{dt} = k_4(SO)(O_2)$$

$$= a_{12}(O_2)^3 + a_{13}(O_2)^2 + a_{14}(O_2) + a_{15}$$

From reaction (6),

$$\text{Rate} = k_6(SO)(O)$$

$$= a_{16}(O_2)^5 + a_{17}(O_2)^4 + a_{18}(O_2)^3 + a_{19}(O_2)^2 + a_{20}(O_2) + a_{21}$$

From reaction (8),

$$\text{Rate} = k_8(S_2O_2)(O_2)$$

$$= a_{22}(O_2)^4 + a_{23}(O_2)^3 + a_{24}(O_2)^2 + a_{25}(O_2) + a_{26}$$

Since reaction (6) is a radical-radical collision process and reaction (8) is an intermediate-reactant process, both cannot be important. Moreover, the rate expressions from both these reactions contain terms of higher order than $(O_2)^3$ whereas the experimental expression is only to $(O_2)^3$. Thus the reaction mainly responsible for sulphur dioxide production must be reaction (4), and the rate is third order with respect to oxygen pressure.

The above mechanism is very similar to that proposed by Norrish[15]. The major differences lie in the initiation step and steps (7) and (8). Without these two steps, no terms in third order of (O_2) can be obtained. Though S_2O_2 has not been found, it is assumed to be an intermediate. Suphur formation is not accounted for, since it is attributed to the reaction

$$2H_2S + SO_2 \longrightarrow 3S + 2H_2O$$

the mechanism of which is unknown. Norrish and his co-workers[15,16] were able to identify the reacting species, except atomic oxygen, but using kinetic spectroscopy, they could not obtain data for the rate dependence on order with respect to each reactant, and they were unaware of the different initiation step in thermal oxidation.

Another plausible mechanism which on stationary state considerations gives for the rate expression one term out of about ten in $(O_2)^3$, is as follows:

Initiation:	$H_2S + O_2 \longrightarrow SH + HO_2$	(1)
Chain propagation:	$SH + O_2 \longrightarrow S\Theta + HO$	(2)
	$HO + H_2S \longrightarrow H_2O + SH$	(3)
Termination:	$S\Theta + SO \rightleftharpoons S_2O_2$	(4)
	$S_2O_2 + O_2 \longrightarrow 2SO_2$	(5)
	$SO + H_2S \longrightarrow H_2O + S_2$	(6)
	$SH \longrightarrow$ wall	(7)
	$HO \longrightarrow$ wall	(8)
	$HO_2 \longrightarrow$ wall	(9)

Since the $(O_2)^3$ term in this mechanism is not important, it is believed unlikely. This mechanism, however, indicates sulphur to be a direct product of H_2S oxidation in addition to being a product formed from the primary product reacting with the original reactant.

In fact, in order to establish whether atomic oxygen is involved, O_2^{36} should be used in mixture with O_2^{32}. From the exchange reaction of

$$O^{16} + O^{18} \longrightarrow O_2^{34}$$

O_2^{34} should be able to be determined mass-spectrometrically. Again, the amount of O_2^{34} produced may be too low to be detected.

The overall activation energy found, 21.2±2k.cal./mole, was in good agreement with the very rough estimate of 18-20 k.cal./mole made by Thompson and Kelland[28]. These authors did not study the thermal oxidation to as low a temperature as the present work and the estimate was very approximate indeed.

If the following values of bond energies are used,

S-H	81.1	k.cal./mole[32]
S-O	118.5	k.cal./mole[30]
O-O peroxide	33.2	k.cal./mole[32]
O-O molecule	118.3	k.cal./mole[32]
O-H	110.6	k.cal./mole[32]
H-OH	118	k.cal./mole[31]

the enthalpies of the reactions (1)-(5) can be estimated to be

Reaction (1)	H = +56 k.cal./mole
Reaction (2)	H = - 3 k.cal./mole
Reaction (3)	H = -37 k.cal./mole
Reaction (4)	H = +27 k.cal./mole
Reaction (5)	H = -30 k.cal./mole.

The overall activation energy of 21.2±2k.cal./mole is smaller than the enthalpy for reaction (1) and indicates that a term $\frac{k_1 k_3}{k_2}$ may be very important in the overall rate constant expression(giving an expected value of 22 k.cal./mole.) This cannot be verified due to the complexity of the rate equation.

REFERENCES

(1) N.M. Emanuel, D.S. Pavlov & N.N. Semenov, Compt. rend. acad. sci. U.R.S.S., 28 618-20 (1940)

(2) N.M. Emanuel, J. Phys. Chem. (U.S.S.R.), 14 863-76 (1940)

(3) N.M. Emanuel, Compt. rend. acad. sci. U.R.S.S., 35 250-5 (1952)

(4) N.M. Emanuel, ibid., 36 145-9 (1942)

(5) D.S. Pavlov, N.N. Semenov & N.M. Emanuel, Bull. acad. sci. U.R.S.S., Classe sci. chem., 98-105 (1942)

(6) N.M. Emanuel, ibid., 221-8 (1942)

(7) N.M. Emanuel, Acta Physiochem. U.R.S.S., 19 360-78 (1944)

(8) N.M. Emanuel, Zh. Fiz. Khim., 19 15-47 (1945)

(9) N.N. Semenov. Bull. Acad. Sci. U.R.S.S. Classe. sci. chem., 210-22 (1945)

(10) N.M. Emanuel, Compt. rend. acad. sci. U.R.S.S., 48 488-90 (1945)

(11) V.G. Marhovich & M.M. Emanuel, Zh. Fiz. Chem., 21 1251-8 (1947)

(12) V.G. Marhovich & M.M. Emanuel, ibid., 21 1259-62 (1947)

(13) N.M. Emanuel, Dokl. Acad. Nauk. U.S.S.R., 59 1137-40 (1948)

(14) P.W. Schenk, Z. Anorg. Chem., 211 150 (1933)

(15) R.G.W. Norrish and A.P. Zeelenberg, Prox. Roy. Soc. Lond., A 240 293 (1957)

(16) A.P. Zeelenberg, 7th Symposium on Combustion, Butterworths, 1959, p. 68

(17) B. de B. Darwent and R. Roberts, Proc. Roy. Soc. Lond., A216 344(1953).

(18) B. de B. Darwent and V.J. Krasnansky, 7th International Symposium on Combustion, Butterworths, 1959, p. 3.

(19) G. Porter, Disc. Far. Soc., 9 60(1951).

(20) D.A. Ramsay, J. Chem. Phys., 20 1920(1952).

(21) e.g. N.V. Sedgwick, The Chemical Elements and Their Compounds, Oxford, 1950, p.980.

(22) R.G.W. Norrish and E.K. Rideal, J. Chem. Soc. Lond., 696 (1923).

(23) S.A. Ryce and W.A. Bryce, Anal. Chem., 29 925(1957).

(24) S.A. Ryce, P. Kebarle, and W.A. Bryce, Anal. Chem., 29 1386(1957).

(25a) M. Kasha, J. Optical Soc. Am., 38 929-34(1947).

(25b) R.E. Hunt and W.J. Davis, J. Am. Chem. Soc., 69 1415(1952).

(26) Handbook of Chemistry and Physics, 41st Edition, 1959-60, Chemical Rubber Publishing Co., Cleveland.

(27) A.V. Jones, J. Chem. Phys., 18 1263(1950).

(28) H. Thompson and N. Kelland, J. Chem. Soc., Lond., 1809(1931).

(29) C.G. Hatchard and C.A. Parker, Proc. Roy. Soc. Lond., A235 518(1956).

(30) R.M. Reese, V.H. Dibeler and J.L. Franklin, J. Chem. Phys., 29 880(1958).

(31) S.W. Benson, Foundations of Chemical Kinetics, McGraw-Hill, 1960.

(32) L. Pauling, Nature of the Chemical Bond, Cornell, 1960.

A P P E N D I X

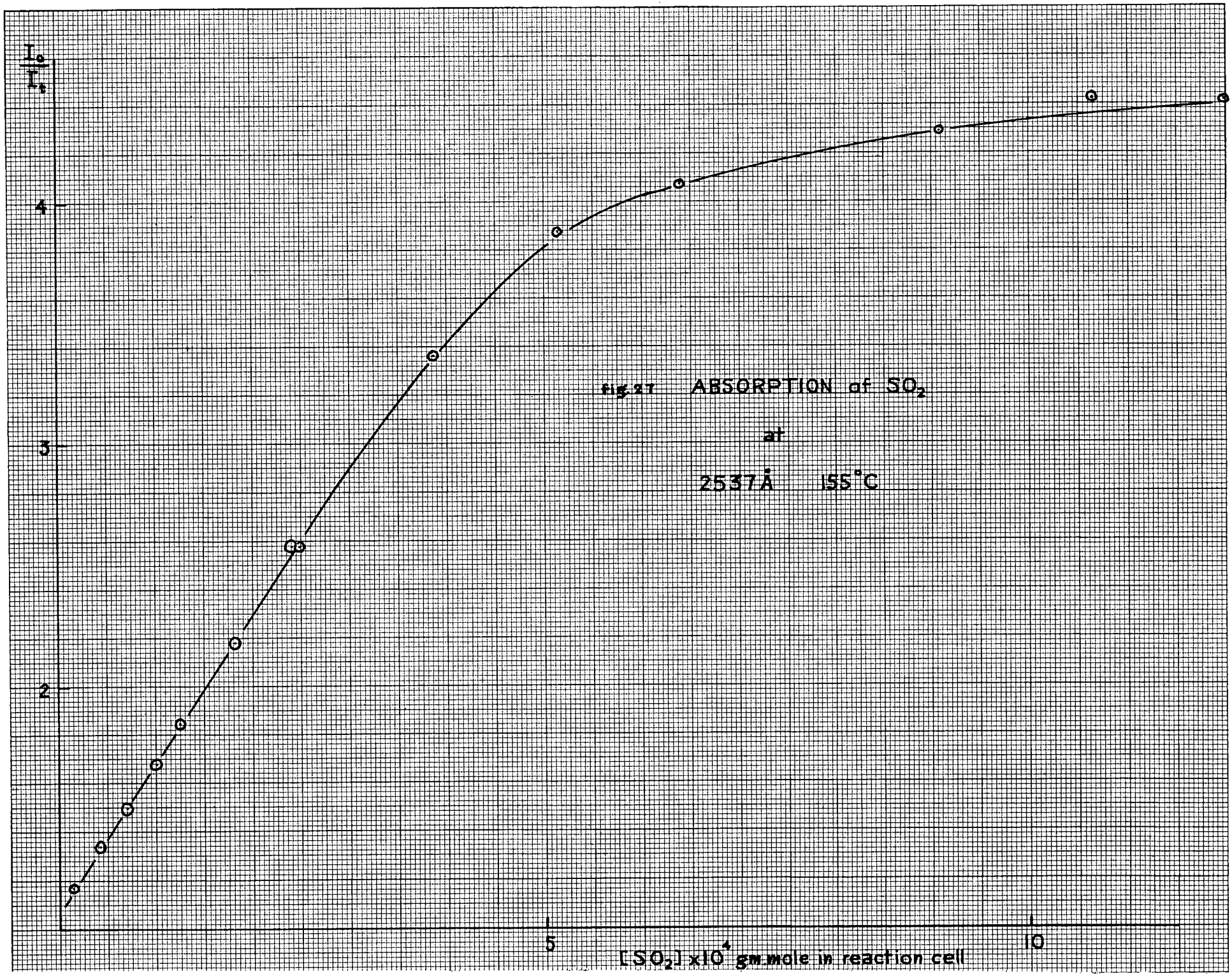

fig. 27 ABSORPTION of SO_2

at

2537Å 155°C

Other results on Photo-oxidation

Expt. No.	Temp. °C	Reaction Time min.	I_o a	P_{H_2S} mm.	P_{O_2} mm.	P_{O_2}/P_{H_2S}	Φ_{SO_2}	Φ_{H_2}
242	150.4	103	2932	8.8	23.1	2.62		1.8
243	150.4	107	2980	7.1	75.1	10.6		2.4
244	135	65	2960	7.1	43;6	6.14		0.78
245	135	75	2940	5.93	45.4	8.13		5.0
246	134.6	102	2920	7.6	44.5	5.85		1.4
247	135	42	2880	7.1	45.8	6.45		-
248	133	212	2550	8.4	79.4	9.45		2.6
249	133	50	2670	13.4	117.3	10.3	266	4.27
265	149.1	316	1860	15.5	30.6	-	-	0.26
276	147.4	124	1980	13.0	37.0	2.84	734	23.2
277	146.1	123	1760	14.3	37.4	2.62	336	9.74
279	146.8	66	1960	12.2	56.2	4.61	282	8.46
280	147.3	199	1930	16.8	46.1	2.75	79	2.4
281	147.5	200	2100	14.3	8.0	0.56	0	4.45
282	148.3	252	1860	12.2	41.1	3.38	2210	40.9
284	147.5	152	1870	20.6	56.6	2.75	680	14.0
285	147.5	352	1540	15.5	4.6	0.30	59	4,55
287	134.0	127	1350	14.3	68.0	4.75	1395	50.2
288	134.6	168	970	16.0	68.0	4.25	3245	57.1
289	137.0	135	2100	13.9	69.7	5.0	2690	37.9
290	137.0	112	2060	26.0	64.3	2.47	2250	9.5
291	136	129	1440	26.0	63.0	2.42	1172	8.0
293	136.6	383	2210	27.3	74.0	2.71	606	10.7
295	135.7	125	1840	17.2	68.9	4.0	1020	28
297	140.2	123	2440	29.4	76.0	2.58	354	12
298	140	335	1570	23.1	70.5	3.0	1020	22
308	149.6	427	413	19.3	197.5	10.4	0	117
310	147.2	120	256	16.8	170.0	10.1	2465	57
319	148.8	127	3780	21.0	121	5.8	109	2.6
320	150.7	282	3680	18.5	122.4	6.6	363	10.2
321	149.0	110	2880	20;5	113	5.5	86	11.2
330	147.0	208	3365	23.5	79.4	3.4	74	6.4
332	149.3	181	3430	21.0	67.6	3.2	64.6	5.6
335	148.2	177	3260	16.4	63.0	3.8	99	11.7
337	152.0	180	2930	19.7	42.0	2.1	30.6	7.7
339	148.7	180	2565	19.7	50.8	2.6	39.4	6.6
340	149.6	253	3020	22.2	45.3	2.0	32.7	6.5
341	147.8	237	2830	21.0	46.1	2.2	22	7.3
343	149.1	233	2980	19.3	37.8	2.0	24	5.9
345	148.3	230	2970	18.5	26.0	1.4	16	6.0

Thermal Oxidation - Effect of Inert Gas at 257°C.

$r = \Delta(SO_2)/\Delta t$ = initial rate in gm.mole/min.

Expt. No.	P_{H_2S} mm.	P_{O_2} mm.	P_{CO_2} mm.	log r
536	18.5	10.9	0	-6.395
532	18.9	15.1	22.6	-6.100
533	19.3	15.0	30.3	-6.306
534	21.4	13.7	37.6	-6.246
535	17.2	4.5	67.2	-6.186